Annu. Rev. Earth Planet. Sci. 1999. 27:75–113

THE GLOBAL STRATIGRAPHY OF THE CRETACEOUS-TERTIARY BOUNDARY IMPACT EJECTA

J. Smit
Department of Sedimentary Geology, Vrije Universiteit, 1081HV Amsterdam, Netherlands; e-mail: smit@geo.vu.nl

KEY WORDS: K/T boundary, Cretaceous-Tertiary boundary, ejecta, tektites, microkrystites, Chicxulub crater, extinction, stratigraphy

ABSTRACT

The Chicxulub crater ejecta stratigraphy is reviewed, in the context of the stratigraphy of underlying and overlying rock sequences. The ejecta sequence is regionally grouped in (*a*) thick polymict and monomict breccia sequences inside the crater and within 300 km from the rim of the crater known from drill holes in and close to the breater, and exposures near the border of Yucatan and Belize; (*b*) Gulf of Mexico region, <2500 m from the crater, with up to 9 m thick, complex, tsunami-wave influenced, tektite-bearing sequences in shallow marine (<500 m deep) environments and tektite bearing, decimeter thick gravity-flow deposits in deep water sites; (*c*) an intermediate region between 2500 and 4000 km from the crater where centimeter thick, tektite-bearing layers occur, and (*d*) a global distal region with a millimeter thin ejecta layer. The distal ejecta layer is characterized by sub-millimeter sized microkrystites, often rich in Ni-rich spinels and (altered) clinopyroxene. Wherever present, the ejecta layers mark exactly the sudden mass-mortality horizon of the K/T boundary. What exactly caused the mass mortality is still uncertain, but it appears the main event leading to the K/T mass extinctions.

INTRODUCTION

It is often surprising how easily the Cretaceous/Tertiary (K/T) boundary can be identified in outcrops and drill cores. Whether in New Zealand, Spain, or the mid-Pacific, the boundary is often visible as a bedding plane. The only

0084-6597/99/0515-0075$08.00

exceptions are deep ocean clay cores and areas with strong bioturbation. This simple observation has far-reaching consequences. In shallow-water sequences, interruptions in sedimentation such as diastems, discontinuities, or disconformities often occur due to sea level changes and tectonic uplift, and a sharp bedding plane is not uncommon. Therefore, it is not surprising to encounter the K/T boundary as a gap in shallow-water sequences.

On the other hand, it is not obvious to expect gaps in deep-water sequences. Before the Deep-Sea Drilling Project (DSDP) and its successor the Ocean Drilling Program (ODP), it was widely believed that sedimentation on the deep ocean floor is more or less continuous. However, DSDP/ODP showed (Van Andel et al 1977, Worsley 1974) that most deep-sea records are also interrupted by omission surfaces ascribed to extremely low sedimentation rates, deepening of the calcium carbonate compensation depth, slumping and contour or turbidity currents. The K/T bedding plane, which also occurs in the deep sea, is therefore often routinely dismissed as representing missing strata and hiatuses produced by sea level changes. However, the sea level chart (Haq et al 1988), which is based on seismic stratigraphy rather than biostratigraphy, does not reveal obvious sea level changes near the K/T boundary to which the bedding-plane discontinuity can be attributed. Also, it is not obvious that important gateways were opened or closed at the time (Figure 1).

A number of deep-water sequences, in particular those near the continental margins, offer continuous records and high sedimentation rates (2–8 cm/kyr). The upper Cretaceous and Paleocene in these sequences are represented by thick packages of strata, usually bedded in cyclic Milankovitch-style patterns (Kate & Sprenger 1993). Such thick packages allow evaluation of the completeness of the K/T boundary transition, through detailed magnetobiostratigraphy and cyclostratigraphy supplemented with other sedimentary evidence at the K/T boundary itself. However, even in these complete sequences, it is hard to prove positively that sedimentation has remained continuous across the bedding plane discontinuity of the K/T boundary.

Controversies exist regarding many aspects of the K/T boundary stratigraphy. It is claimed that the upper Cretaceous record shows evidence of a gradual trend or change toward the K/T boundary, likely the result of deteriorating climate leading to extinctions. If such a trend is real, it may be difficult to make a distinction between (mass) extinctions related to the gradual trend and mass extinctions related to the consequences of the impact event itself.

The K/T impact ejecta-layer stratigraphy is also controversial in several aspects. It is widely believed that this layer is the result of a large meteorite impact because of the global association with an iridium anomaly, shocked minerals, and impact spherules, but alternative views also exist, mostly related to volcanism (Officer & Page 1996). The conflicting evidence seems to result

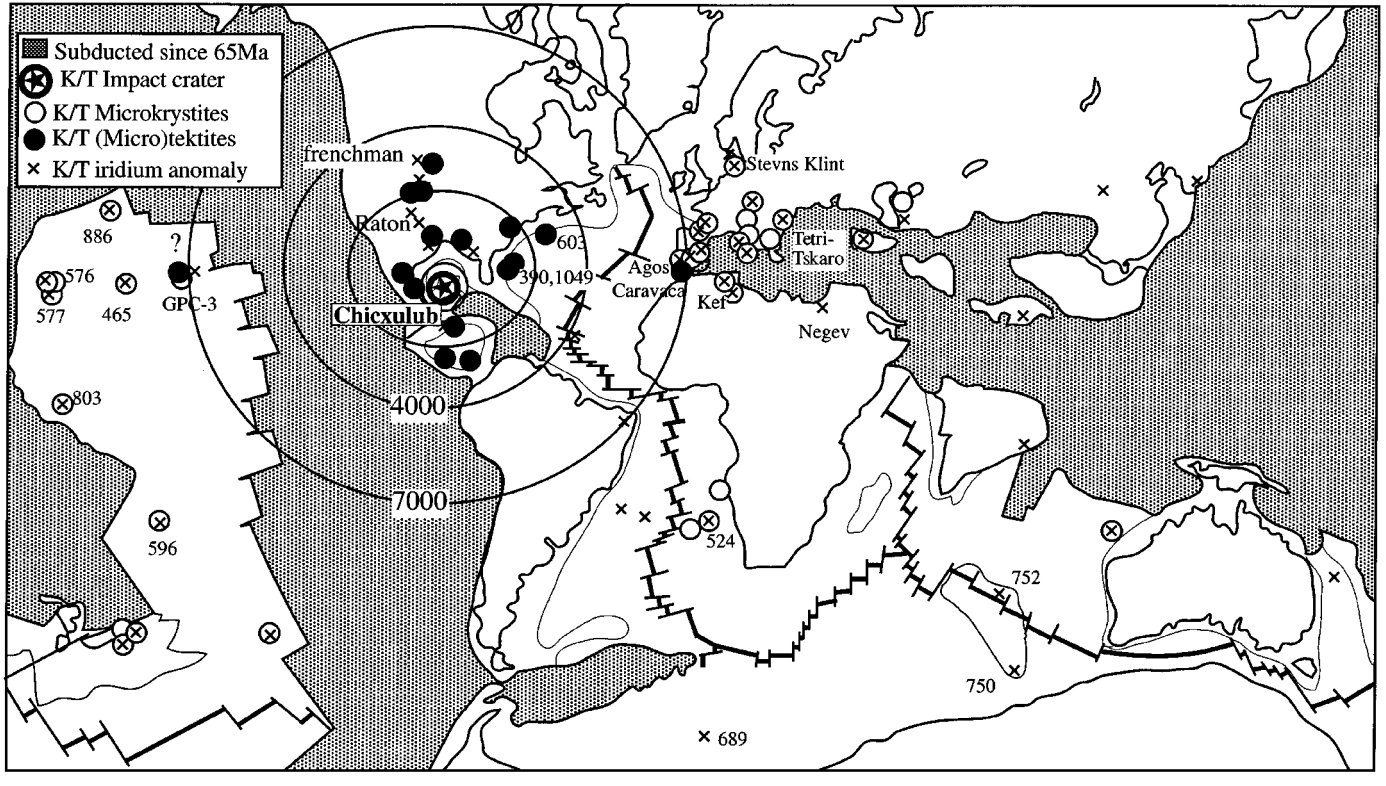

Figure 1 Distribution of K/T ejecta, projected on a paleogeographic map at 65 Ma. Distances of proximal, intermediate, and distal ejecta layers are 2500, 4000, and 7000 km, respectively. Numbers are ODP/DSDP sites.

from the complete alteration of the layer and the frequently strong bioturbation, which has led to different interpretations of the ejecta products.

Four types of ejecta deposits can be distinguished: (*a*) the distal settings, global in scale, where an ejecta layer that is a few millimeters thick has survived, (*b*) the continental Western Interior, with 1- to 2-cm-thick ejecta layers in coal-swamp deposits, (*c*) the Gulf of Mexico region, associated with high-energy clastic deposits, and (*d*) ejecta blanket deposits, up to 3.5 crater radii away from the crater rim.

In this paper I review the global stratigraphy of the K/T boundary ejecta deposits in chronological order in relation to the information provided by the sediments deposited before and after the ejecta layer. I first review the stratigraphy of the upper Maastrichtian. Next, I discuss the many aspects and disguises of the ejecta layer in each of the four regions mentioned above. Finally, I examine the first deposits of the basal Paleocene that provide the information on the biotic and environmental consequences of the Chicxulub impact.

K/T BOUNDARY DEFINITION

For a better understanding of the K/T boundary events and their controversies, it is essential to understand the historical and official definition of the K/T boundary.

Most geologists associate the K/T boundary with mass extinctions, and the definitions of the stratotypes of the Maastrichtian and the Danian stages are not in conflict with this view. The Danian, erected by Desor (1846), is the senior stage and was followed as much as possible in the definition of a new K/T boundary stratotype. The base of the Danian stratotype section is located at Stevns Klint in Denmark; at the base it includes the K/T boundary clay known as the "Fiskeler." The ejecta layer was later (Alvarez et al 1980) shown to be present at the base of the clay. The ejecta layer is part of the Fiskeler (Christensen et al 1973) and, therefore, the K/T boundary is located below the ejecta layer (Figure 2).

The International Commission on Stratigraphy (ICS) (Cowie et al 1989) has defined the new K/T boundary Global Stratotype Section and Point (GSSP) in the El Haria formation in outcrops west of the town of El Kef in Tunisia, based on the abundant presence of well-preserved calcareous and organic-walled microfossils and the unusually complete and expanded section. The upper Maastrichtian and Paleocene are more than 500 m thick and consist predominantly of drab hemipelagic calcareous marls with a few micritic limestone intervals. Obvious breaks in sedimentation or hard grounds are absent in the entire interval. The K/T boundary is marked by a reddish 2-mm-thick layer, the ejecta

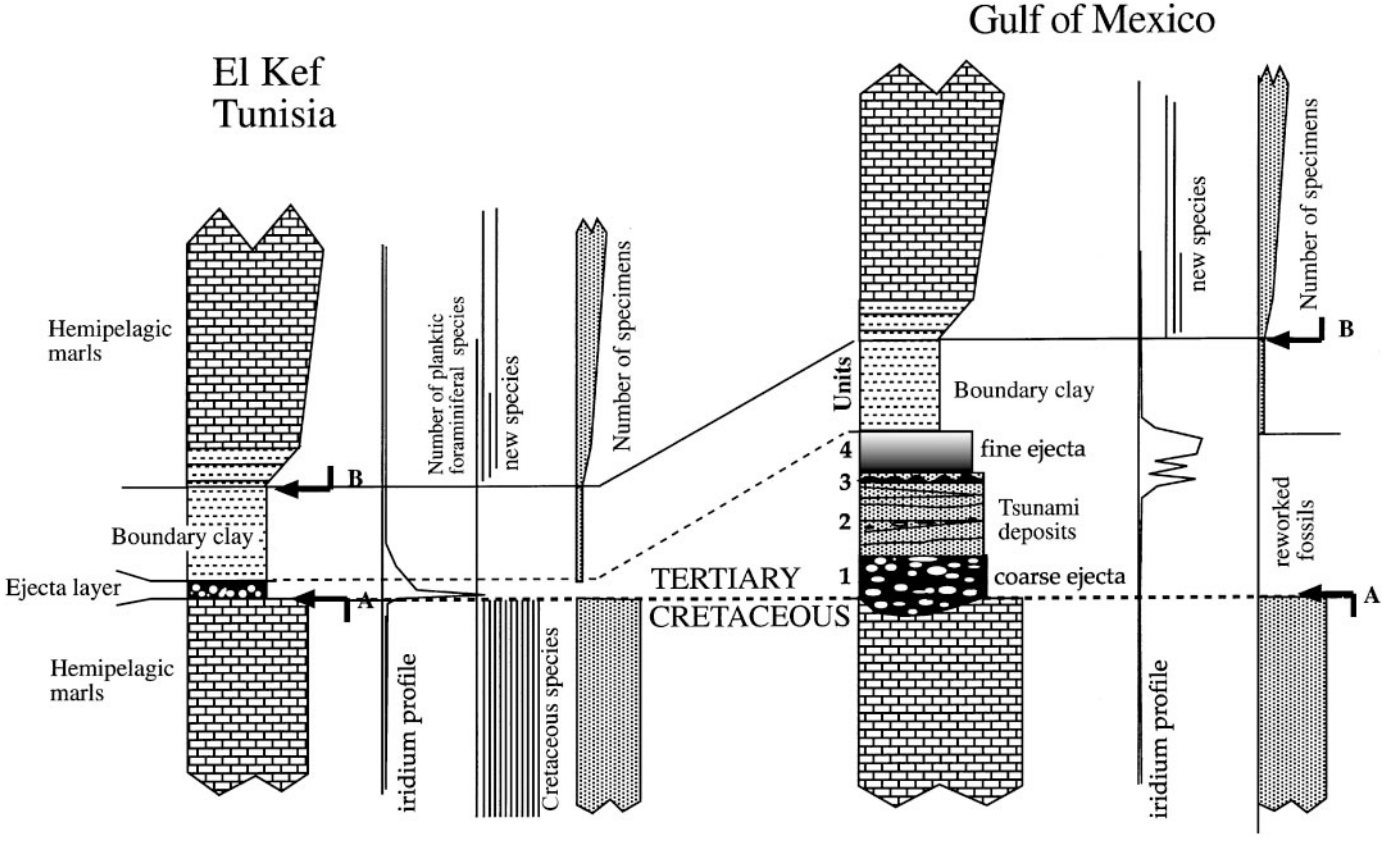

Figure 2 Schematic stratigraphy of the K/T boundary stratotype section at El Kef, compared with the proximal unit I-IV sequence in the Gulf of Mexico. In distal sites, iridium profile and other types of ejecta coincide; in proximal sites these are separated vertically. (*A*) Mass-extinction level. (*B*) First occurrence of new planktic foraminiferal species.

layer, immediately overlying calcareous marls with abundant Maastrichtian calcareous microfossils. The ejecta layer is enriched in iridium and contains shocked quartz and nickel-rich spinels (Robin et al 1991), as well as altered microkrystites (Smit & Romein 1985). The red ejecta layer is directly overlain by the K/T boundary clay, a 25-cm-thick clay interval, extremely poor in calcareous microfossils. In line with the Danian stage, the ICS commission placed the K/T boundary GSSP below the ejecta layer. The GSSP is an instant in time, represented by the bedding plane between the red ejecta layer and the fossiliferous marls below the boundary. All other criteria (such as the mass-extinction level, last occurrence of Maastrichtian fossils, first occurrence of Paleocene fossils, iridium anomaly, microkrystites, microtektites, soot, impact diamonds, amino acids, and negative shift of $\delta^{13}C$ and $\delta^{18}O$) are closely associated and can be used for correlation but are not part of the K/T boundary definition.

This definition is not inaccurate for the majority of distal K/T localities because all ejecta peak in the same thin layer. Problems occur in defining the K/T boundary around the Gulf of Mexico because the different types of ejecta (tektites, iridium anomaly) are at differenct stratigraphic levels (Gartner 1996, Keller & Stinnesback 1996, Keller et al 1994, Smit et al 1994) (Figure 2).

UPPERMOST CRETACEOUS (LATE MAASTRICHTIAN)

Open-ocean pelagic carbonate sequences with slow sedimentation rates are often incomplete or condensed. The most complete upper Maastrichtian sedimentary sequences occur in outer-shelf sections, in particular along the former Tethys ocean. Examples included in this review are the sections of Agost (Groot et al 1989), Caravaca, and the Bay of Biscay region (Zumaya) in Spain (Smit & Romein 1985); Bottaccione in Italy (Luterbacher & Premoli Silva 1964); and El Kef in Tunisia (Keller 1988, Nederbragt & Koning 1994). Those sections are in pelagic to hemipelagic facies and contain rich foraminiferal and nannofossil faunas and floras and insignificant amounts of macrofossils—usually echinoids, inoceramids, ammonites, and numerous trace fossils. There is no evidence for hard grounds or omission surfaces that abound in typical shallow-water sections, e.g. on the Gulf of Mexico coastal plain, Stevns Klint, and the Maastricht area.

There are a number of ways to determine the temporal sequence of events relevant to the K/T boundary. Because of the abundance of microfossils and the ease of use, traditional biostratigraphy is most frequently used but is often hampered by diachronous datum levels and facies depth dependence of faunal assemblages, which mask global biotic changes.

The late Maastrichtian is represented by the *Abathomphalus mayaroensis* foraminiferal biozone, which is subdivided by three datum levels near its

termination (entry of *Pseudoguembelina hariaensis* and *Plummerita hantkeninoides* and exit of *Gansserina Gansseri*; Pardo et al 1996). The first appearance of *A. mayaroensis* is at about 2 Myr below the K/T boundary in low latitudes and, at up to 4.5 Myr in high latitudes (Huber 1992). Planktic foraminiferal faunas remain rich and diversified throughout this interval; the zone has the highest species richness of the Cretaceous. Considering the length of the zone, remarkably few evolutionary changes occur in this interval. Whether a number of large ornamented tropical species disappeared less than 15 kyr before the K/T boundary, thus before the Chicxulub impact event, as claimed by Keller (1988, 1996), is still debated. A blind-test effort at the K/T type section near El Kef did not yield a definitive answer (Keller 1997, Smit & Nederbragt 1997). However, all the disappearing species were still found just below the K/T boundary by at least one of the blind-test participants.

Nannofossil biostratigraphy is not better suited for zonation of the late Maastrichtian. Low-latitude marker species either are absent at high latitudes or are as diachronous as planktic foraminifers. The species traditionally used for defining the base of the Tertiary (*Biantholithus sparsus, Biscutum romeinii, B. parvulum, Criciplacolithus primus*) are shown to be already present in the Maastrichtian (Romein et al 1996), although their size is much smaller. The most reliable criterion for defining the K/T boundary using nannofossils is the relative abundance of so-called persistent or disaster species above the K/T boundary clay (Gartner 1996, Percival & Fischer 1977).

A magnetostratigraphy has been established for a few well-known sections, (Gubbio, Caravaca, Agost, Bjala), but a reliable magnetostratigraphy for the upper Cretaceous of the Biscay region or El Kef (Kate & Sprenger 1993; Moreau et al 1994, 1989; Roggenthen 1976; Lindinger 1989) could not be established. Yet magnetostratigraphy may provide a better estimate than biostratigraphy for completeness of sections (Kent 1977). The K/T boundary occurs in magnetochron C29R, with a duration presently estimated at 833 kyr (Berggren et al 1995). Earlier estimates are considerably less, 570 kyr (Berggren et al 1985). To assess the size of the gap, or amount of time involved in the K/T interval, sedimentation rates can be linearly extrapolated upward and likewise downward to the K/T boundary (Figure 3). The estimated time involved to deposit both Cretaceous and Tertiary intervals within C29R is more than the total time allowed for C29R and may indicate an increased sedimentation rate in the vicinity of the K/T boundary interval, rather than the time involved in the K/T interval. In another approach, the orbital cyclicities measured in the K/T interval could be used (Herbert & D'Hondt 1990, Kate & Sprenger 1993). Berger et al (1989) calculated the duration of the precession periods at 65 Myr ago at 18.7 and 22.5 ka, respectively, averaged at 20.65 ka. In C29r, at least 14 cycles are observed in the Cretaceous (Agost) and 15 in the Paleocene (Zumaya) (Kate

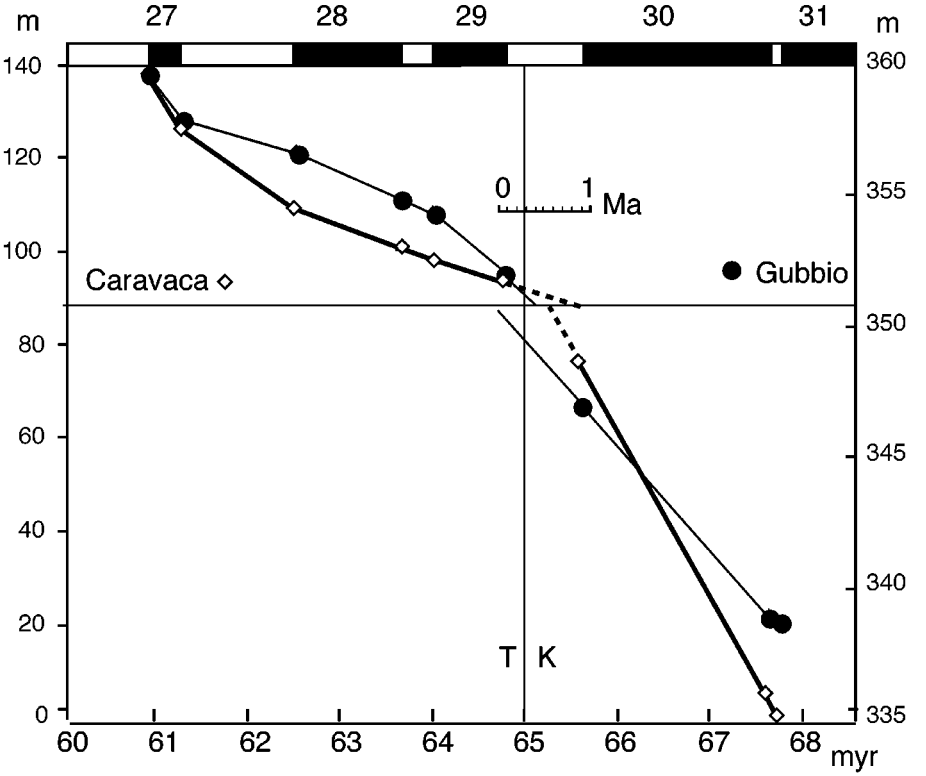

Figure 3 Accumulation rates of (*filled dots*) Gubbio and (*diamonds*) Caravaca, based on magnetostratigraphy (Chrons 27–31), extrapolated toward the K/T boundary. The misfit at the K/T boundary indicates (*a*) increased sedimentation rate in C29R, (*b*) an understimation of the duration of C29R. No significant gaps at the K/T boundary are expected.

& Sprenger 1993), using the above cycle lengths, accounting for 542.3 and 652.5 kyr, respectively, averaged at 594.5 kyr. This would better fit the earlier (Berggren et al 1985) estimate of 570 kyr. However, if the recent estimate of 833 kyr is valid, there may be a gap: at least eight precession cycles appear to be missing, contrary to the results from simple extrapolation. This contradiction raises questions about either the applicability of astronomical cycles or the length of C29r determined from seafloor magnetic anomalies.

The lithology of the complete continuous sections shows major cyclic lithological variations (0.5–2 Myr) in the Maastrichtian that are probably related to sea level change. The lithological succession at Zumaya, which is more or

less the same in all the Bay of Biscay sections, compares well with the sections in Agost and Caravaca in Spain and El Kef in Tunisia, indicating that these changes are probably eustatic.

The more calcareous, lithified parts of the sections occur in the base of the upper Maastrichtian, in the middle, and near the top, about 13 cycles below the K/T boundary. Although the carbonate content in these limestone intervals is higher, the thickness of the observed precession cycles is less, showing a reduced flux of both clay and pelagic carbonate. These intervals probably represent sea level highstand to maximum-flooding stages, in good agreement with the studies on benthic foraminifers (Pardo et al 1996) (Figure 4).

Deformation of the uppermost Cretaceous strata is noticeable in regions close to the Chicxulub crater. The strata underlying the ejecta layers often show signs of soft-sediment deformation, whereas strata overlying the ejecta

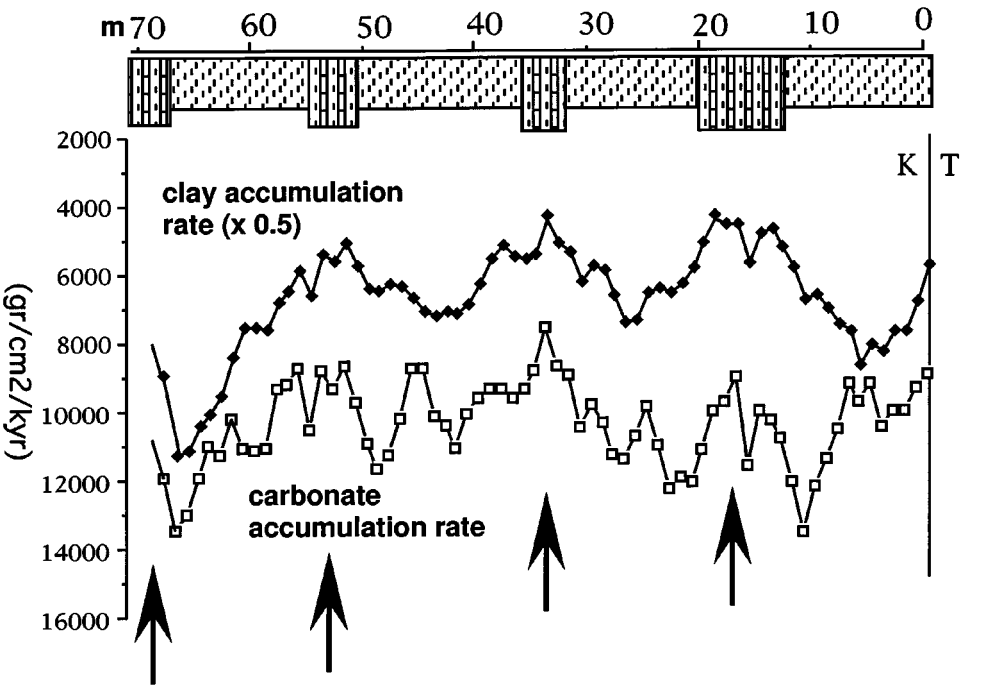

Figure 4 Accumulation rates of carbonate and clay, calculated on the average duration and thickness of the observed precession cycles (Kate & Sprenger 1993) for Zumaya section, Bay of Biscay region, Spain. Arrows indicate maximum flooding surfaces. The flooding surface at 70 m may correspond to the 67.5 ma maximum flooding surface from Haq et al (1988).

layers are undisturbed. This phenomenon is particularly striking on the Blake Nose, Florida. Sediments of ODP Site 1049 directly underlying the ejecta layer are tightly slump-folded, whereas the overlying stratigraphy is undisturbed and shows the normal biostratigraphic succession. This is also visible on the seismic facies interpreted from the seismic profiles across Blake Nose. The same large-scale slumping of the upper Cretaceous is inferred from the lithology at and seismic profiles across DSDP Sites 536 and 540 (Alvarez et al 1992b, Buffler et al 1984), but again the lower Paleocene is undisturbed. In outcrops around the Gulf Coast, upper Cretaceous soft-sediment deformation has been frequently observed (Smit et al 1996). An intriguing example is the Moscow Landing, Alabama outcrop. Normal faulting, with associated soft-sediment deformation of the Maastrichtian chalk, began slightly before the emplacement of ejecta but continued through deposition of the ejecta and associated clastic beds, which are presumably emplaced by tsunami waves. The slumping is confined to strata below the ejecta layer, but the faulting continued into Paleocene, as indicated by the offset of the overlying burrowed transgressive surface and thickness differences of the same lithologic units on either side of the fault planes. Slumping has also been observed in the Mimbral, Rancho Nuevo, and Cuauhtemoc outcrops in northeastern Mexico (Alvarez et al 1992a) before or during emplacement of the ejecta (tektites). Large-scale slope failures are inferred from the lithological successions in Bochil (Chiapas) and El Caribe in Guatamala. All these phenomena indicate deformation and large-scale slope failures related to seismic energy input from the Chicxulub impact itself, some of it induced before the emplacement of the ejecta from the same impact event (Figure 5).

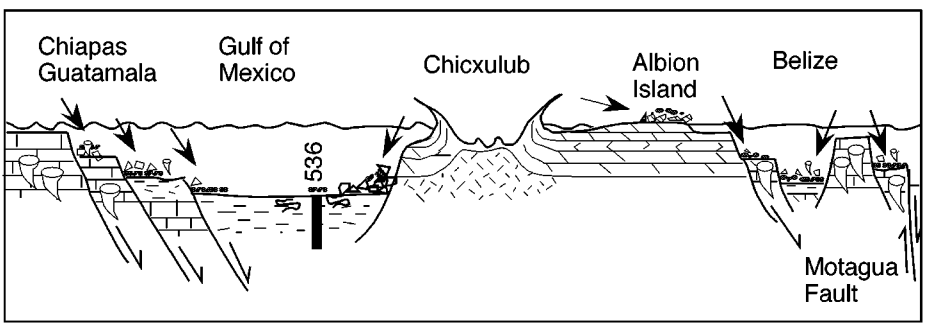

Figure 5 Schematic cross section through the Chicxulub crater and surrounding dolomite or rudist-bearing carbonate platform margins with possible impact triggered slope-failure features (not to scale).

Transition Upper Maastrichtian Ejecta Layer

In complete distal sections, the K/T transition is additionally marked by a characteristic burrowed, but not completely bioturbated, horizon in the top of the Maastrichtian. The burrows are conspicuous, typically filled with dark clayey material from the clay layer above the K/T boundary. In particular, the Tunisian sections (Kef, Elles) (Smit et al 1997), those in Spain (Agost, Caravaca) (Smit 1977), and the Furlo and Petriccio sections in Italy (Montanari et al 1983) contain a well-preserved trace-fossil fabric. Sediments above and below the K/T boundary are bioturbationally well mixed. The sequence of trace-fossil fabrics across the K/T shows a significant decrease precisely at the K/T boundary. This means, indirectly, that bottom life also decreased dramatically in these (outer) shelf sections at intermediate (200–1000 m) water depths (Figure 6). As premium for K/T boundary studies, the ejecta layer in these sections is therefore stratigraphically undisturbed. Nevertheless, burrow traces of *Chondrites*, *Planolites*, and *Zoophycos* have often scavenged the ejecta layer, because the burrows are filled with impact spherules (Kotake 1989). The scavenging of the ejecta layer obviously caused enhanced concentrations of iridium in the upper 10 cm of the Maastrichtian and a decrease in iridium in the ejecta layer

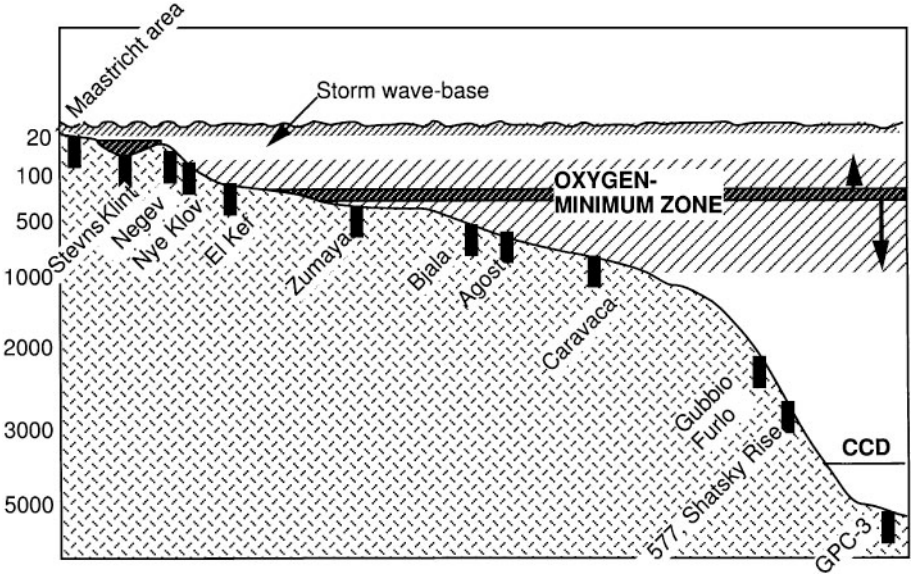

Figure 6 Depth of deposition in meters of distal K/T boundary sites, as estimated from various sources. Hatched areas and arrows indicate the presumed expansion of the oxygen minimum zone directly after the impact event.

(Montanari 1990). All ichnofossil types found are typical for burrowing of soft, muddy substrates. It is often mentioned that the discontinuity at the K/T boundary may indicate an erosion or hard ground surface, but evidence of these mud burrowers does not support this view.

The ejecta layer is not well preserved in open-ocean deep-water sections such as DSDP Site 577 (Michel et al 1985) and abyssal clay cores such as GPC-3 (Kyte et al 1996, 1993). Also, the K/T boundary interval in the Negev sections Ein Mor and HorHaHar is completely bioturbated, leading to a smearing that extends the iridium anomaly and first and last occurrences of foraminifers. Sediments across the K/T interval are saturated with ichnofossils, and numerous body fossils of crustaceans, notorious burrowers, occur below and above the boundary.

The top few centimeters of the Maastrichtian just below the ejecta layer are characterized by dissolution, creating the illusion of a period of transition toward the ejecta layer. At El Kef, only internal casts of foraminifers are preserved in this interval. In addition, in Agost and Caravaca the $CaCO_3$ content is lowered. In the Apennine sections (Gubbio, Furlo, Petriccio), the surfaces bounding the ejecta layer are obviously stylolithic, indicating diagenetic dissolution. At Stevns Klint, so-called dissolution horse-tail structures occur below the ejecta layer. Most of the dissolution has a diagenetic character, most likely the result of leaching by sulfuric acid produced by dissociation of the abundant pyrite framboids in the K/T boundary clay.

K/T EJECTA LAYER

The ejecta layer at the K/T boundary shows distinct characteristics related to distance from the Chicxulub crater. Those sites that possess a thick >3-cm layer containing (altered) tektites of impact glass, characterized by a distinct bubbly texture (Figure 1), are labeled proximal. These sites occur mainly in the Gulf of Mexico, the Caribbean, and the east coast of the United States up to New Jersey (Olsson et al 1997), DSDP Site 603 (Klaver et al 1986) up to 2500 km from the crater center. Continental North American sites, ranging in distance from 2200 km (Raton Basin) (Izett 1990) to 4000 km (Alberta) (Carlisle et al 1991) and ranging in thickness from 0.5 to 2 cm, are labeled intermediate and partially owe their characteristics to the coal-swamp depositional environment. Sites at a distance of 7000 km and greater are labeled distal and are characterized by an ejecta layer thickness of only a few millimeters that contains abundant microkrystites (Smit et al 1992a).

Distal Sites

At sites more than 7000 km from the Chicxulub crater, the thickness of the ejecta layer, when properly reconstructed, is fairly constant at not more than 2–3 mm

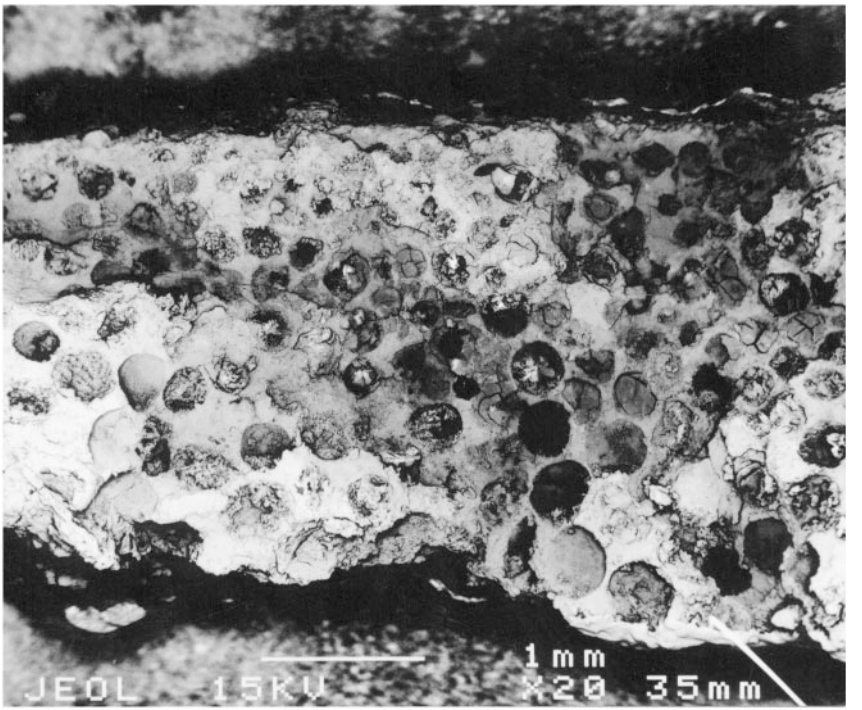

Figure 7 SEM image of the distal ejecta layer, showing graded spherule layer altered into an early diagenetic goethite concretion that is highly enriched in iridium (86 ng/g), compared to the ejecta non-concretionary clay adjacent to the concretion (2 ng/g). Tetri-Tskaro, near Tbilisi, Republic of Georgia.

(Figure 7). Owing to variable degrees of compaction and local resedimentation, it is not possible to reconstruct a reliable thickness distribution as a function of distance from the impact crater. The site with an undisturbed ejecta layer closest to the Chicxulub crater is Alamedilla in Spain, some 7000 km away, and the most distal site is Woodside Creek in New Zealand, now about 15,000 km away. The ejecta layer thickness at both sites is a few millimeters thick. The distal ejecta layer is invariably altered, and at some sites only components such as high-temperature magnesioferrite spinels, shocked minerals, impact diamonds, and, thus far only at DSDP site 577, Ca-rich clinopyroxene (augite) have survived diagenetic alteration (Figure 8) (Smit et al 1992a).

The stratigraphic distribution of the different components in the ejecta layers is determined mainly by differences in settling velocity and thus in grain size. In the Tetri-Tskaro section in Georgia the microkrystites are clearly graded (Figure 7). In a water column exceeding a few tens of meters, grain size

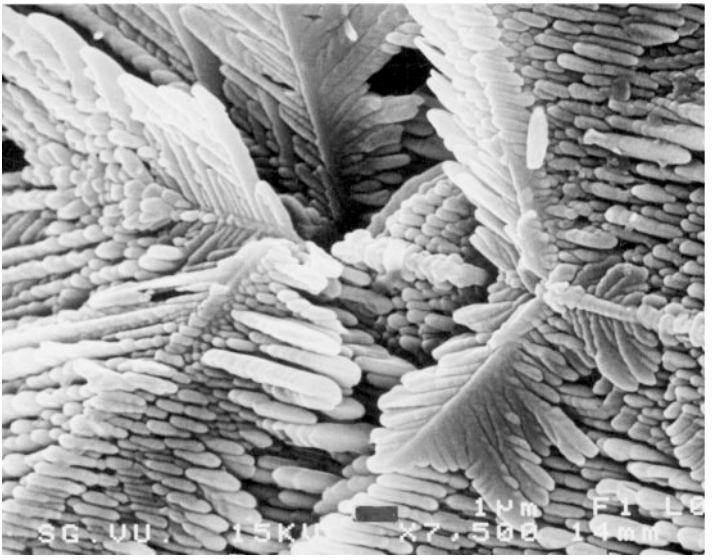

Figure 8 SEM image of clinopyroxene (augite) dendrites, from a microkrystite of the K/T boundary of DSDP Site 577b. Interstitial glass has been etched out by seawater.

distribution is determined by differential settling and does not yield information about arrival times of the different ejecta or help determine whether one or more simultaneous impacts occurred at the K/T boundary, as suggested by Robin et al (1993). In the Petriccio section (Montanari 1990), smaller-size shocked minerals are concentrated in the lower part of the ejecta layer, contrary to the distribution of shocked minerals in the ejecta layer in the western interior of the United States (Izett 1990). A position below the peak of the (larger) microkrystites is difficult to explain by settling of ejecta from one impact. However, as in the other Appennine K/T sections, the ejecta layer and overlying boundary clay in the Petriccio section appear to be well mixed, favoring redistribution by sedimentary processes over two impact events.

The most abundant, macroscopically visible components in the distal ejecta layer are spherules with a relict crystalline texture (Smit et al 1992a), designated microkrystites (Glass & Burns 1988). These microkrystites are restricted to the ejecta layer, except where dispersed by bioturbation. The microkrystites cannot be easily classified in terms of a simple mixing of different compositional end-members, as is the case for the more proximal tektites (Sigurdsson et al 1991), because there is no compositional data owing to ubiquitous alteration of the layer. A proxy for composition may be the mineralogy, inferred from

the relict crystalline texture. It is possible to distinguish several groups of microkrystites within one ejecta layer at one site. Microkrystites are altered to goethite in Stevns Klint, Denmark, to As-rich pyrite in Zumaya, to potassium feldspar in Caravaca, and to glauconite in Fonte d'Olio, Italy (Montanari 1990, Smit et al 1992a), but owing to the different diagenetical and (micro) chemical environments, it is doubtful that the distinctions between sites reflect meaningful differences in original composition. Different groups in a single sample can be distinguished in Agost and Caravaca, Spain; Furlo and Petriccio, Italy; and DSDP Site 577 (Pacific). One microkrystite group is characterized by skeletal Ni-rich magnesioferrite spinels (Kyte & Bostwick 1995), embedded in a dark smectitic matrix containing ghosts of olivine crystals. Another group consists dominantly of K-spar, with skeletal-texture pseudomorphs after clinopyroxene and plagioclase (Montanari et al 1983, Smit et al 1992a). A third group of green glauconite microkrystites in some places contains skeletal K-spar crystals. The latter two groups do not contain magnesioferrite crystals and may represent mixing between two end members. Do the two groups (with and without spinels) represent different chemical compositions or a different cooling history? The spinel-bearing group is clearly more mafic in composition and significantly enriched in iridium (Montanari et al 1983); the other two groups, glauconite and K-spar rich, are not. Therefore, it is likely that the spinel-bearing microkrystites are formed from the hotter parts of the ejecta vapor cloud (Kyte & Bostwick 1995) containing a larger proportion of the bolide than the other, clinopyroxene-rich microkrystite type.

Several features associated with the composition and global distribution of the Ni-rich magnesioferrite spinels are not easily explained. Most K/T spinels located in the Pacific and a few in the South Atlantic (DSDP Site 524) and Indian Ocean (ODP Site 761) have significantly higher MgO, Al_2O_3, and Fe_2O_3/FeO content than do spinels from the Tethys and show myrmekitic intergrowth with, presumably, Ni-rich periclase (Mg, Ni, Fe) O, indicating formation at extremely high temperatures (Kyte & Bostwick 1995). At a finer regional scale, there are considerable differences, particularly in Cr content among the European sites. The asymmetric global distribution may support oblique impact. The high Fe_3/Fe_2 ratio in all magnesioferrite spinels, but in particular in the Pacific spinels, requires a relatively high oxygen fugacity during crystallization. Interaction with atmospheric oxygen is usually inferred: one hypothesis (Robin et al 1993) posits the formation by ablation of many bolides at relatively low altitudes, whereas another hypothesis (Kyte & Bostwick 1995) suggests atmospheric mixing of part of the impact vapor cloud. The Robin et al (1993) hypothesis seems inconsistent with the uniform composition over a large area and with the periclase inclusions, whereas the Kyte & Bostwick (1995) hypothesis seems inconsistent with the observation that impact ejecta (microtektites)

are usually highly reduced. Probably related to this problem is the high oxidation state of the impact glass found at Beloc, Haiti, and Mimbral, Mexico (Jehanno et al 1992, Oskarsson et al 1996). Although atmospheric interaction may play a role, liberation of oxygen from the vaporized CO_2- and SO_3-rich evaporitic and carbonate sedimentary cover from the Chicxulub target area, as suggested by Oskarsson et al (1996), cannot be excluded.

The number of microkrystites can be estimated in some sections with an undisturbed ejecta layer (Agost, Caravaca, Tetri-Tskaro). In these sections the ejecta layer remains constant in thickness along the outcrop for at least 50 m. In other sections, diagenesis and bioturbation prevent an accurate estimate. Basically, the ejecta layer consists of a dense packing of spherules, 250 μm in mean size, yielding about 20,000 microkrystites per square centimeter. There is no reason to believe that the distribution elsewhere is much different. Woodside Creek, New Zealand; the Pacific sites GPC-3 and DSDP Site 577; South Atlantic (DSDP Site 524); and Stevns Klint yield hundreds of microkrystites per cubic centimeter. The total number of microkrystites, assuming a global coverage of comparable microkrystite density, is 1×10^{23} microkrystites or a volume of about 850 km^3 deposited in distal sites alone.

Between 4000 and 7000 km from the crater, there are very few data from K/T ejecta layers, although GPC-3 may occur in this range. Kyte et al (1996) and Smit et al (1992a) note the occurrence of smooth hollow clay spherules, sometimes with splash forms, without relict crystalline textures, in GPC-3 and ODP Site 886. Ruiz et al (1992) report goethite spherules and droplets with similar morphology from Agost, and recently I found droplets at Alamedilla, Spain (J Smit, unpublished data). Because of the similarity to the altered spherules from Dogie Creek and the Gulf Coast, these droplets are interpreted as altered tektites and indicate that in the North Pacific and Spain, tektites and microkrystites occur together in the same ejecta layer.

Intermediate Sites

The ejecta layer in intermediate sites, 2000–4000 km from the Chicxulub crater, is represented by a couplet of claystone layers in continental deposits, invariably coal-swamp deposits now turned into coal or lignite. At sites where the K/T transition, as determined by palynostratigraphy, occurs in overbank deposits, the ejecta layer has been spread out over several decimeters and is no longer visible as a layer. The reported thickness of the ejecta layer varies from 2 cm in Raton Basin (Izett 1990), Red Deer River (Lerbeckmo et al 1996), and Dogie Creek (Bohor et al 1987) to 0.5 cm in the Seven Blackfoot coulee in Montana and near Frenchman River in Saskatchewan (Lerbeckmo et al 1996). There is no clear relation of thickness to distance from Chicxulub, although, in general, the thickness in the Raton Basin is consistently around 2 cm. A thickness around

1.5–2 cm in Montana and Canada seems a local maximum, but 0.5 cm is the average.

The ejecta layer has a distinct, dual-layer stratigraphy, consisting of a thick, lower claystone layer, often sharply separated from a thinner upper layer. The lower claystone layer is often termed the kaolinitic layer (Bohor et al 1987) or K/T boundary claystone (Izett 1990), and the upper layer is often termed the fireball, magic, or K/T boundary impact layer because it contains high iridium concentrations and the bulk of the shocked minerals. The lower claystone layer is composed mainly of kaolinite, and the upper layer is mainly composed of a mixture of kaolinite and illite/smectite mixed-layer clays. The dual stratigraphy extends from Brownie Butte in Montana (Bohor et al 1984) to Raton Basin in New Mexico. Izett (1990) showed clearly that the lower claystone has signs of reworking because of the presence of detrital clastic grains and vitrinite particles and the discontinuous, lenticular nature of the layer. Additionally, the lower claystone layer at Dogie Creek, Wyoming, a site where the layer almost entirely consists of goyazite spherules, is clearly cross-bedded.

It has been argued that the dual-layer stratigraphy represents two different impact events. If so, these have to be almost simultaneous because both layers, though separate, are amalgamated. Not even a single season of fallen leaves separates the layers. Reported discontinuities, truncations of root traces, and cutoffs of pumice fragments of glass can be explained by sedimentary processes during emplacement of both layers. The evidence for reworking in the lower layer suggests that the emplacement of the lower layer was affected by disturbances in the shallow-water coal swamp, possibly induced by the blast loaded with tektites. On the other hand, because of its continuous thickness, the upper layer seems to result from relatively quiet settling of fine impact debris through the atmosphere.

Proximal Ejecta Sites

The proximal sites <2500 km from the Chicxulub crater (Figures 9, 10, and 11) can be roughly subdivided into five types: (*a*) sites near the Atlantic continental margin and Atlantic Coastal Plain that contain mainly graded tektite deposits, (*b*) shelf to outer shelf locations around the Gulf of Mexico at relatively shallow <500 m depths, (*c*) sites around the carbonate platform in Chiapas, Guatamala, and southern Belize, (*d*) deep-water sites in the Gulf of Mexico and the Caribbean, and (*e*) ejecta-curtain deposits in and close to the Chicxulub crater, extending to northern Belize.

ATLANTIC COASTAL PLAIN AND CONTINENTAL MARGIN The ejecta layer near the Atlantic coast consists of a single, 3- to 17–centimeter-thick, often graded layer of greenish spherules. The morphology of the spherules, including splash

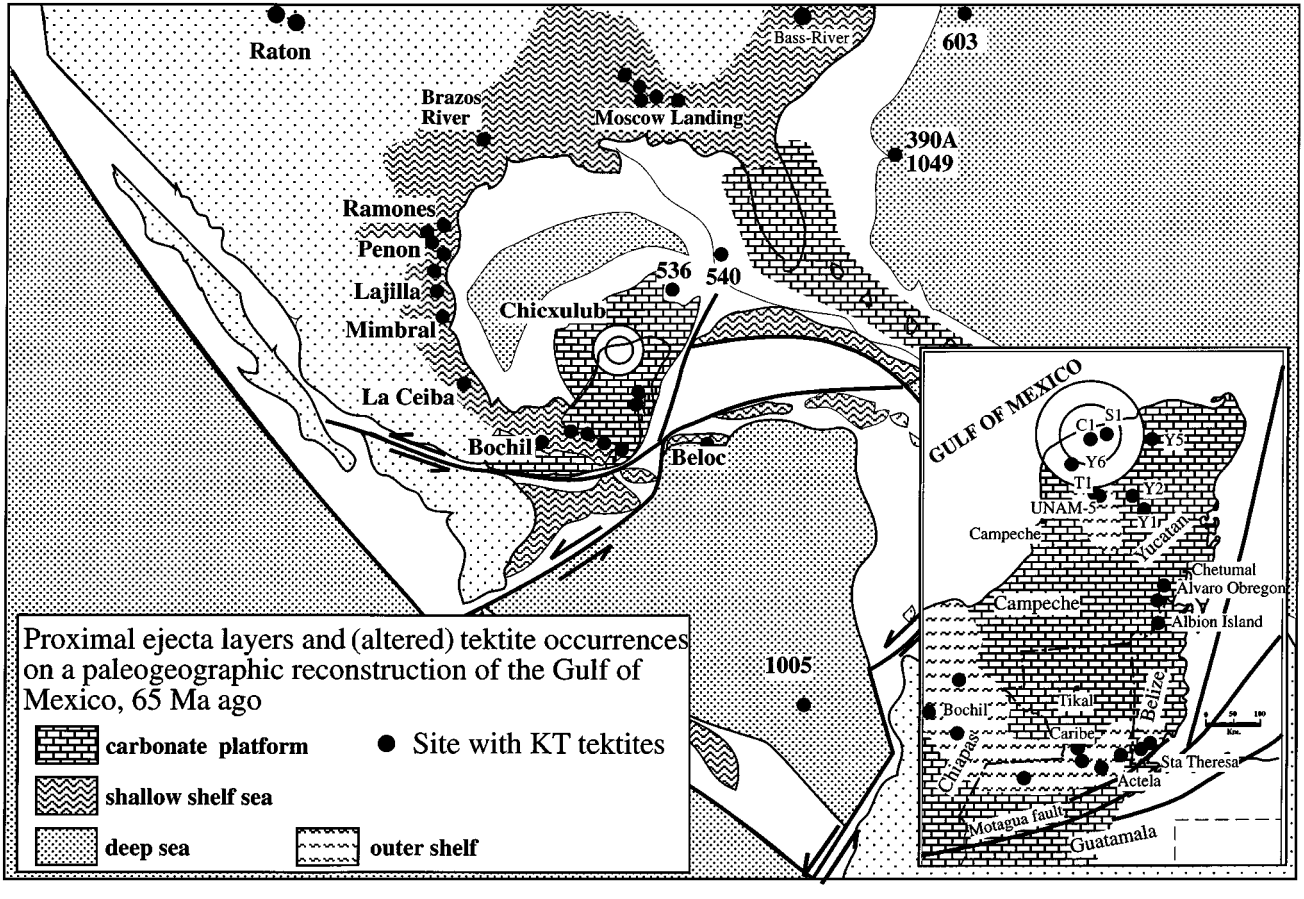

Figure 9 Paleogeographic map of the Gulf of Mexico and Yucatan with the proximal sites discussed in the text. Numbers are DSDP/ODP sites.

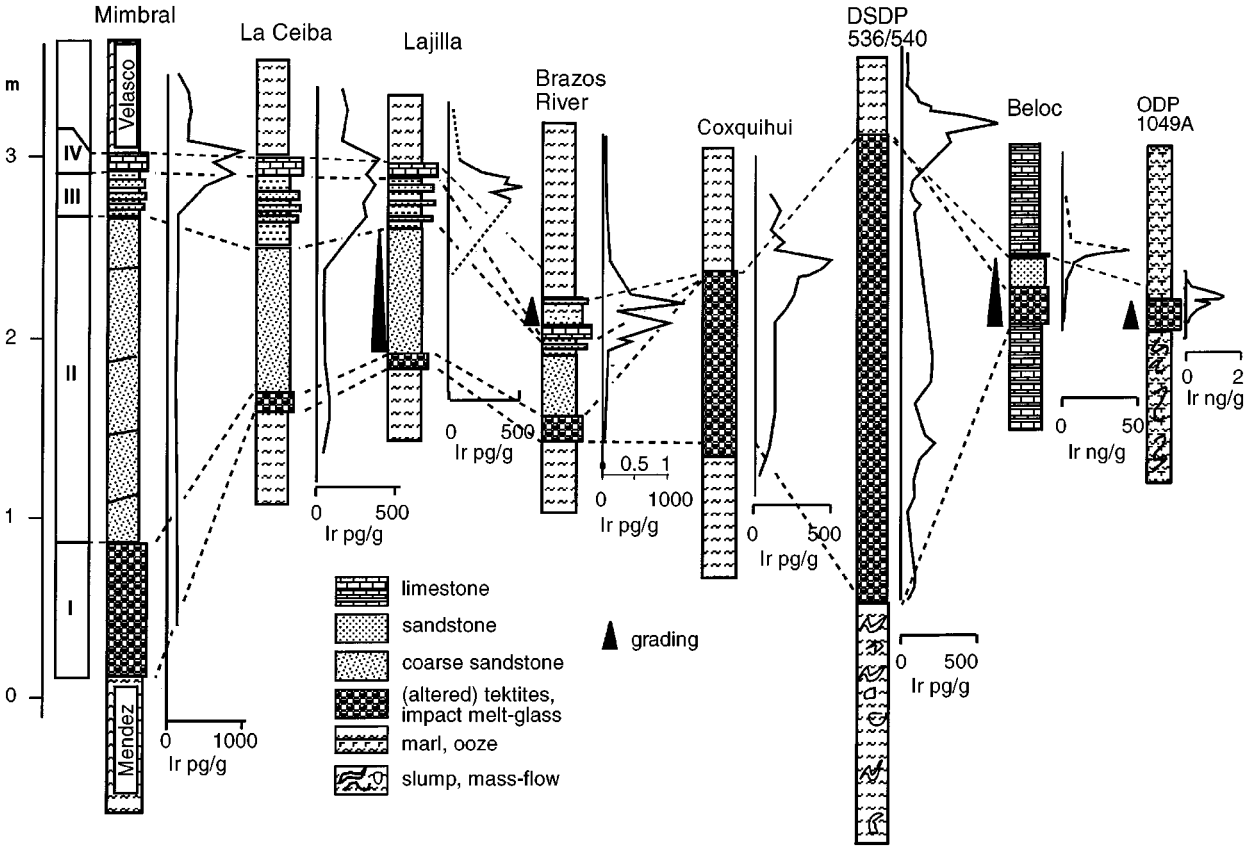

Figure 10 Scheme of the stratigraphy of the proximal sites with measured iridium profiles discussed by region in the text. The Ir data are from F Asaro and P Claeys (personal communication), except La Lajilla and ODP Site 1049 data are from R Rocchia (unpublished data). Roman numerals I to IV indicate the subdivisions of the clastic beds with evidence for tsunami waves (Smit et al 1996). Coarse ejecta, mostly altered tektites, are consistently separated stratigraphically from the fine ejecta indicated by Ir.

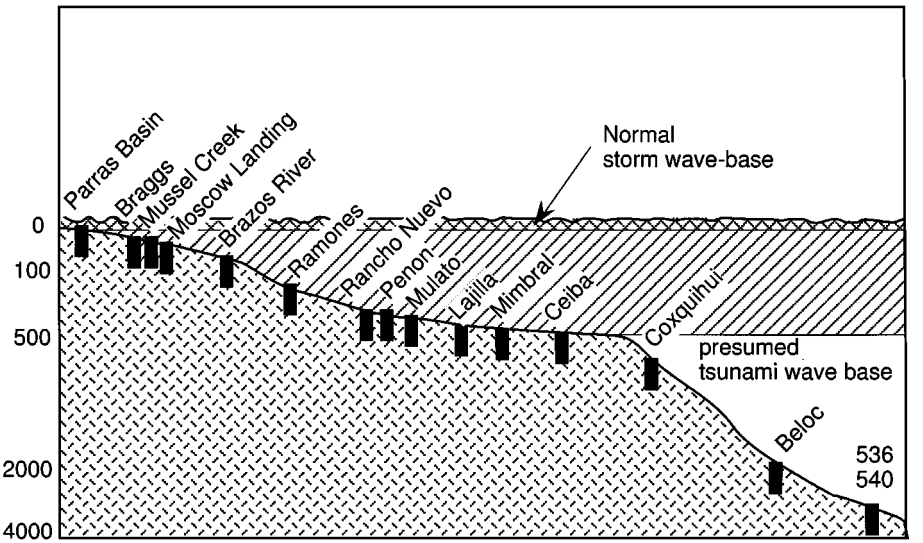

Figure 11 Depth of deposition of the proximal sites discussed in the text. *Hatched area* is the estimated tsunami-wave base. *Cross-hatched area* is the normal storm-wave base.

forms with flow banding and abundant internal vesicles (Klaver et al 1986), is identical to the spherules with a preserved tektite glass core from Haiti (Izett 1991, Sigurdsson et al 1991) and the goyazite spherules from Dogie Creek.

The distinction between the Atlantic and the intermediate sites at 2000–2500 km is somewhat arbitrary. Main differences are the deposition in a marine environment and the slightly greater thickness (>3 cm). A dual-layer stratigraphy is not observed but, as noted above, should not be expected here from a single impact. Mean spherule (tektite) size is about equal: 0.95 mm in Dogie Creek (Bohor et al 1987) and 1.1 mm in Bass Creek (Olsson et al 1997) and DSDP Site 603 near New Jersey (Klaver et al 1986). In ODP Site 1049 (a redrill of DSDP Site 390A), a single 7- to 17-centimeter–thick graded layer of green spherules (<2.3 mm) is observed, capped by a red layer. The abundantly present Cretaceous foraminifera in the graded ejecta layer suggests that the grading did not result from differential settling through the water column but from a gravity flow. Iridium concentrations are enhanced throughout the layer but, in particular, are enhanced just above the spherule layer (not in the red capping), again indicating that the spherule layer has been remobilized after deposition. Clear evidence for tsunami wave activity has not been found in any of the sites, although Olsson et al (1997) report large clasts in sediments overlying the ejecta layer.

GULF OF MEXICO COASTAL PLAIN These sites are invariably characterized by a complex set of clastic sandstones, containing coarse ejecta at the base and an iridium anomaly at the top. The sites extend from Moscow Landing in Alabama to La Ceiba, a site east of Mexico city and renamed Tlaxcalantongo by Stinnesbeck et al (1996). Smit et al (1992b, 1996), Stinnesbeck et al (1993), and Stinnesbeck & Keller (1996) subdivide the set from bottom to top into three macroscopically visible units (Figure 12). A fourth unit is discernible only after detailed grain size analysis (Smit et al 1996). Bohor (1996) compares the subdivision with a classical, idealized Bouma Ta-Te sequence.

The depositional environment of the U.S. Gulf Coast is in a shallow shelf sea. In eastern Mexico, it is in a deep outer shelf, according to the lithology and foraminiferal assemblages in the underlying Maastrichtian sediments (Figure 11).

The lowermost unit I is characterized by channeled, poorly sorted, coarse-grained pebbly sandstones containing flat rip-up clasts, abundant spherules interpreted as (altered) tektites, and limestone particles interpreted as unmelted limestone ejecta (Smit et al 1996). The unit displays low-angle cross bedding, often lateral accretion-type channel infill. The channels are mostly discontinuous. The matrix between the spherules and clasts consists primarily of planktic foraminifera that have been winnowed from the surrounding seafloor.

Unit II is composed of a series of upward thinning and fining lenses or extended sheets of finer-grained, well-sorted calcareous sandstone. The lenticular bodies are more extended than the channels from unit I, but lateral channel infill structures have not been recognized. Lithic clastic grains are more frequently found in unit II than in unit I, but the dominant component of the sandstones are planktic foraminifera. Locally, plant debris has accumulated in layers. Rounded, armored mud balls, the armoring consisting of tektite-like spherules, are frequently found at the base.

At Mimbral, up to six, stacked and imbricated lenticular sandstone layers were recognized, each with a clearly coarse basal part containing tektite-like spherules, probably reworked from unit I. Each layer has eroded into the top of the underlying sheet, producing disconformities. In La Lajilla and El Penon, where the outcrops can be traced over several hundreds of meters, about eight sheet-like, thinning-upward sandstone bodies were identified.

Unit II displays numerous sedimentary structures that are particularly well developed at La Lajilla (Figure 12). These structures include parallel laminations with associated primary current lineation, lunate, linguid, and climbing ripples. More than 200 individual current directions measured in several locations in unit II (Brazos River, Rancho Nuevo, El Peñon, La Lajilla, Mimbral, and La Ceiba) indicate bimodal current directions in each of the locations. Often the dominant directions differ by almost 180° (Smit et al 1996).

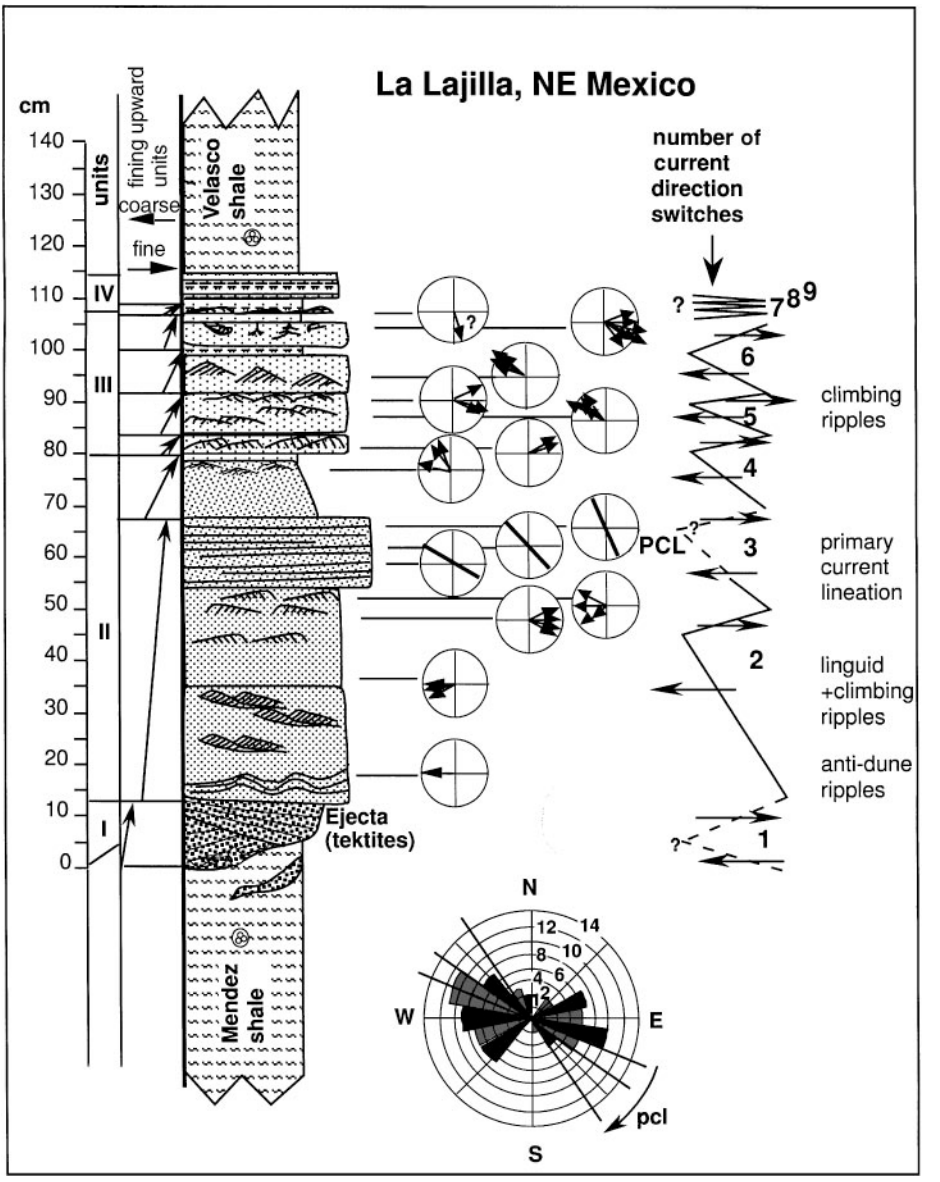

Figure 12 La Lajilla, northeast Mexico. Lithology of K/T clastic beds is subdivided in units I to IV. The fining-upward units, types of sedimentary structures, and measured current directions are indicated. Primary current lineations (PCL); 1–9 indicate the approximate number of current direction changes, assumed to indicate the passage of successive tsunami waves.

The transition between units II and III is defined by the first of a series of alternating soft, thin silt layers and thin, rippled, fine-grained sandstone layers. These silty layers are the lowermost layers enriched in iridium, although the highest iridium concentrations occur in the graded silt layers above the highest rippled sand layer.

The current directions measured in the ripples remain variable, again often differing by 180°. The rippled sandstone layers are sheet-like and continue over the entire outcrop; at La Lajilla and El Peñon, they continue over at least 150 m. The upper two to three layers contain diverse burrow traces, mostly confined to the surface of the sandstone layers. The ichnoassemblages are tiered, that is, a different assemblage is found on each successive level. *Chondrites* occupy the deeper levels; different types of *Zoophycos*, *Planolites*, and *Rhizocorallium* occupy the upper levels. One type of burrow, consisting of straight 1-cm–diameter tubes, extends down to the lowest silt layer from unit III, and approximately 1 m below the top of the highest ripple layer in straight vertical burrows, before spreading out horizontally into the silt layer in huge, 3-m-long, radiating, often bifurcating burrows. All these ichnofossils can be explained by colonization after deposition of the entire clastic unit and do not necessarily indicate a considerable length of time between deposition of sand layers. Keller et al (1997) mention burrows in layers from units I and II. However, a number of flame structures were found in the base of the same layers, where mud has been squeezed into the bottom of the sand layer by loading. These could have been mistaken for burrow traces.

Unit IV, the highest unit, is silty and varies in thickness on top of the last observed sandstone layer. Bralower et al (1998) label this unit the K/T boundary cocktail because of the abundance of a mixture of reworked microfossils and ejecta. Unit IV is often visible in outcrop because it forms a conspicuous, more lithified micritic layer of 5–10 cm thickness, which has been mistaken locally for a Cretaceous (Mendez formation) shale layer, probably because it consists largely of reworked material from the underlying Mendez shale (Keller et al 1997). A detailed grain size analysis (Smit et al 1996) has shown, although it is not apparent in outcrop, that this unit is size graded, and therefore originated from the settling of fine resuspended material. Iridium concentrations are highest in this fine-grained graded unit, indicating that the fine-grained iridium carrier settled at the same time.

Origin of the Clastic Layers

The clastic layers are interpreted differently. Smit et al (1996) interpreted the complex of layers as a result of the interaction of large tsunami waves, produced by the Chicxulub impact. Although the impact itself did not occur in the deep ocean basin of the Gulf of Mexico, a large part of the ejecta curtain, presumably thousands of cubic kilometers, fell in the Gulf, and slope failures along

the Campeche escarpment may additionally have triggered tsunamis. Keller & Stinnesbeck (1996) and Stinnesbeck & Keller (1996) interpreted the layers as the result of a sea-level lowstand followed by transgression, or of repeated gravity-flow deposits related to eustatic sea level changes over thousands of years during the uppermost Maastrichtian. Bohor (1996) also interpreted the layers as a result of gravity flow deposits, not extended in time but as one coherent gravity-flow event triggered by the Chicxulub impact. He considered the lithological succession as comparable with a single idealized Bouma sequence. Stinnesbeck & Keller (1996) based their view on an alternative position of the K/T boundary, above the clastic layers, and the presumed presence of burrow fabrics and "normal hemipelagic layers" in, between, and above the sandstone layers. In their view, because thousands of years passed between deposition of the tektites in unit I and the iridium in unit IV, they proposed two impacts, the lower of the two related to the Chicxulub impact, the other at the K/T boundary. However, the grain size distribution of these normal hemipelagic layers is clearly different from, and coarser-grained than, undisputed upper Maastrichtian and Paleocene normal hemipelagic layers. Also, because the burrows in the lower units could not be confirmed, their interpretations are in question—particularly the claim that thousands of years would have passed between deposition of individual sand layers.

Bohor's (1996) view of the clastic units as a single turbidite is at odds with the frequent hydrodynamic jumps indicated by the grain size shifts at each successive layer and the reversed current directions. Moreover, the grain size distribution related to the specified Bouma intervals is different from that in a classical turbidite. Although hydrodynamic jumps may occur occasionally in composite turbidites, the complex K/T sequence is not comparable with any turbidite sequence in well-studied flysch basins. Also, repeated reversals of current directions are never observed in a single turbidite and are difficult to explain by gravity-flow mechanisms.

A problem with the interpretation of Smit et al (1996) is the great distance from the presumed coastline. It is difficult to imagine how large-scale oscillatory water movements, although triggered by exceptionally large waves, can transport material, including clastic sand grains and wood fragments, from a coastline at least tens of kilometers away. The oscillatory movements are necessary to explain the measured reversals in current direction, so reworking by tsunami waves is at least involved in part of the story. However, the transport of near-coastal material to the locations farther into the gulf may be partially a consequence of gravity flows.

Chiapas, Guatamala, and Southern Belize

The sites in Chiapas, Guatamala, and southern Belize all occur on or around the Yucatan-Chiapas carbonate platform and incorporate very coarse mass flows

underlying an iridium anomaly, sometimes associated with altered tektite-like spherules (Montanari et al 1994, Stinnesbeck et al 1997). A typical sequence is the Bochil section in Chiapas, where a 70-m-thick graded mass flow, containing >5-m-sized platform limestone blocks often with rudists and miliolids, occurs at the K/T boundary. The matrix of the mass flow contains a mixture of deep (bathyal) and shallow water biota, such as planktic foraminifers, miliolids, orbitoids, and rudists. The absence of any dolomite or anhydrite blocks, which constitute the dominant components in the ejecta blanket/curtain sites, for example, in northern Belize and Yucatan, indicates that these blocks are not ejecta from the Chicxulub impact ejecta curtain but represent local mass wasting from the edge of the carbonate platform. The coarse, often conglomeratic, mass flows are overlain by a graded sandstone deposit, followed by a thin rusty silt/mudstone layer. The top of the sandstone and the thin, fine silt/mudstone contain an iridium anomaly and numerous shocked quartz grains. Shocked quartz (J Smit, unpublished data) and enhanced iridium concentrations (E Fourcade et al 1998) are also present in the El Caribe (Guatemala) section directly above the graded mass flow. Stinnesbeck et al (1997) describe four sections in Guatemala where platform limestone facies underlie a breccia unit with spherules, which is itself overlain by outer-neritic to upper bathyal pelagic sediments of basal (P1a) Paleocene age, indicating an abrupt subsidence of a few hundred meters.

Recently, a new site with tektite-like spherules and splash forms was found in southern Belize, near Santa Teresa. These features occur in green boulders, a (minor) component in a conglomerate of dominantly Cretaceous shallow-water limestone pebbles, rudists (*Barrettia* sp.) and boulders of brown pelagic marls with a well-preserved lower Paleocene P1a foraminiferal assemblage. The geological setting is complicated by the block faulting related to movements along the nearby Motagua fault, separating the Chortis and North American plates and active in late Cretaceous and early Paleocene times (Figure 5). The tectonic activity has repeatedly triggered mass flows in grabens adjacent to highs with platform limestones. Most of these mass flows are not related to the Chicxulub impact.

Beloc (Haiti), Coxquihui (Mexico), and DSDP Sites 536/540

Beloc (Haiti), Coxquihui (Mexico), and DSDP Sites 536/540 are located in deep water, between 600 and 3000 m (Figure 10), and do not contain evidence for tsunami waves in the coarse-grained K/T ejecta deposits.

In Coxquihui, the K/T ejecta deposits are a 90-cm-thick, poorly graded sandstone bed consisting of three cross-bedded sublayers. The components are almost exclusively vesicular spherules of calcite. Iridium contents are elevated throughout the layer but are most enriched in the top. This site, although only

30 km from La Ceiba, is either too deep to have been influenced by the tsunami waves or too far away from the coastline for clastic sands to reach the site. The overlying and underlying pelagic marls are reddish colored, suggesting deposition below the oxygen minimum zone (>600 m) in contrast to the other eastern Mexican outcrops, and contain a fauna with deepwater style planktic species (large *Globotruncana contusa*, *G. stuarti*).

The Beloc, Haiti site is famous for the content of vesicular glass cores inside spherules (Figure 13), droplets, and 1-2 cm blebs with rims of smectite. Beloc is still the only site known, besides the rare occurrence in Mimbral and La Lajilla in Mexico, where the impact glass is abundantly present.

The physical, isotopic, and chemical properties of the glass have been treated by Blum (1992), Izett (1991), Jehanno et al (1992), Koeberl (1992), Koeberl

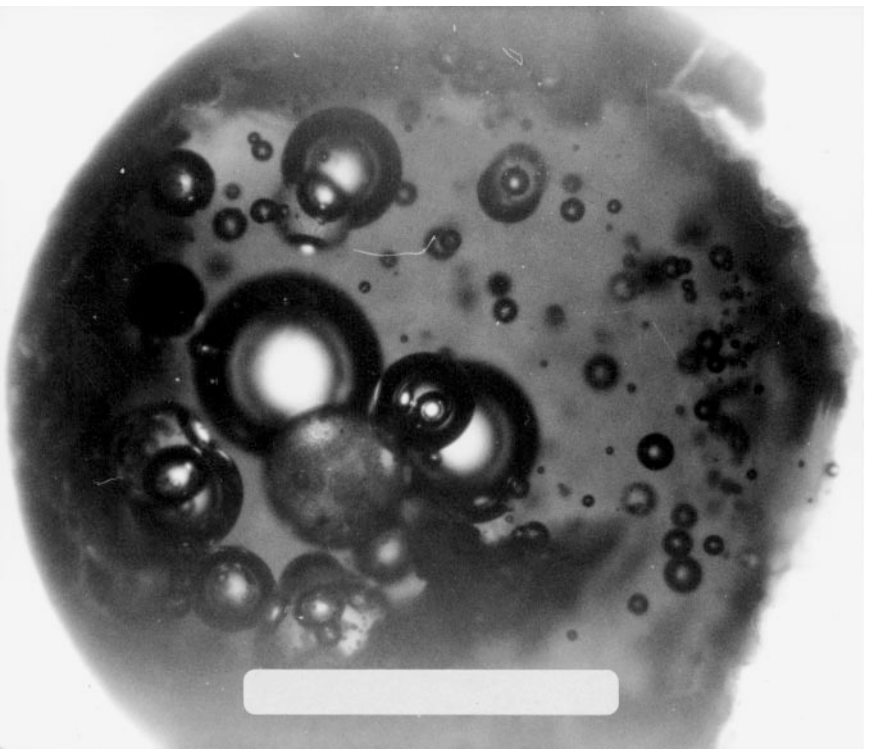

Figure 13 Thin section of round tektite consisting of brown, low-CaO glass, from the M site of Beloc, Haiti. The vesicles, when cracked and immersed in a liquid, appear to be almost at vacuum pressure. This vesicular texture is usually inherited through pseudomorphosis and provides a fingerprint for the recognition of Chicxulub ejecta. Scale is 1 mm.

& Sigurdsson (1992), Kring & Boynton (1991), Maurasse (1991), Oskarsson et al (1996), Sigurdsson et al (1991), and Swisher et al (1992), and I highlight only some of the more important features. The glass has two end-member compositions: a light, yellowish CaO (<31%) and MgO—rich to dark brown and relatively CaO (~5%) and MgO poor. These compositions probably reflect the amount of dolomite/limestone dissolved in the glass. Some CaO-rich glass contains sulfur, and some does not, reflecting different mixtures of anhydite and limestone. The trace-element composition of the brown glass is similar to the composition of the melt inside the crater (Y6-N17) (Figure 14). Some glasses show schlieren (Figure 15) of both end-member compositions in one single

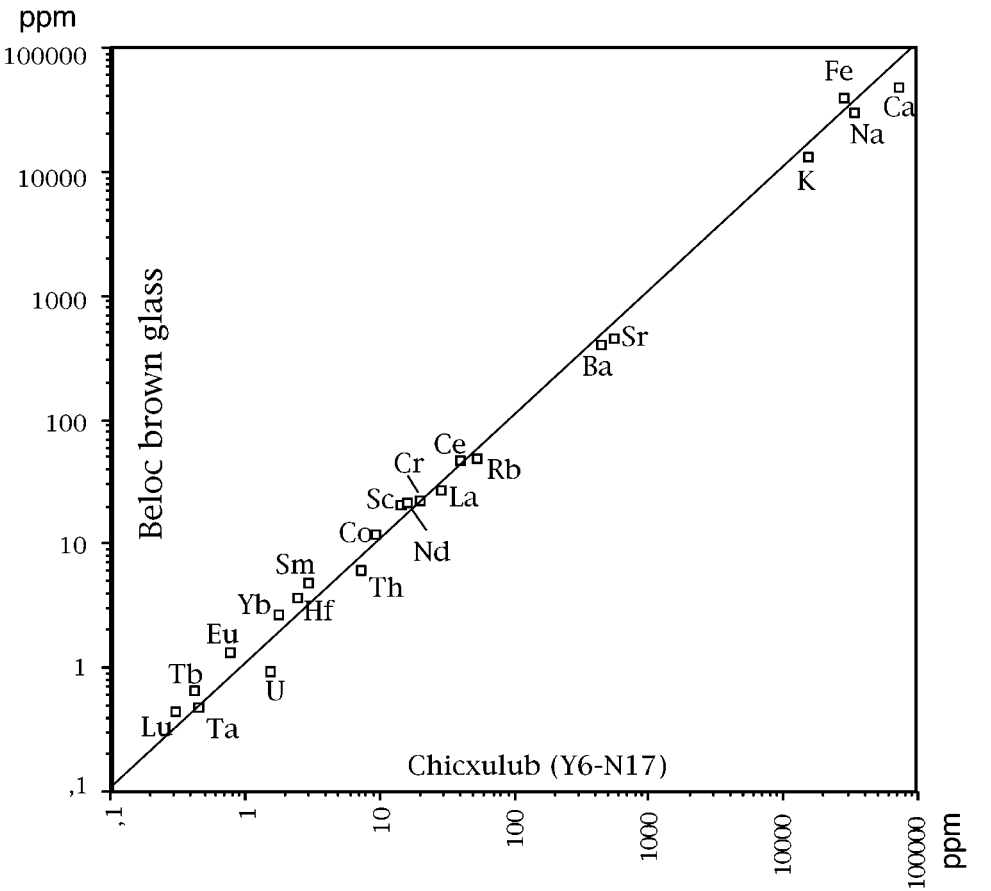

Figure 14 Comparison of trace-element compositions of the glass matrix of sample Y6-N17 from drill core Yucatan-6 in the Chicxulub crater, with the brown, low-CaO glass from Beloc, Haiti.

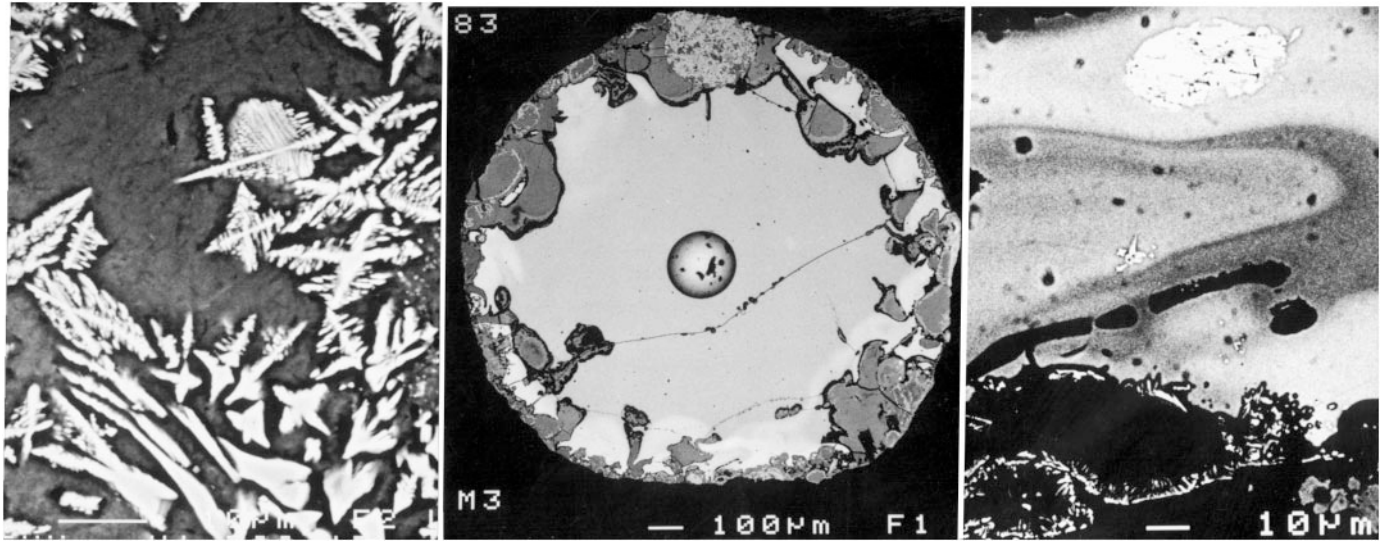

Figure 15 Backscatter SEM image of a complete glassy tektite (M site, Beloc, Haiti) with only marginal alteration to smectite at the rim (*center*). The rim is characterized by CaO-rich glass, in schlieren, that contains pockets of a melilite crystal meshwork (*left*) and unmelted inclusions of anhydrite (*right*). SEM scanning of a 2-cm large fragment of the ejecta layer with more than 60 individual tektites, where each tektite still has at least a glass core (*left*), shows that >50% of tektites have such a melilite and CaO-rich rim.

spherule. On the surface the schlieren are often differentially etched by weathering. Such schlieren are also visible on completely altered spherules of other proximal sites (DSDP 603, Dogie Creek, Mimbral) (Izett 1991). Lyons & Officer (1992) suggested that only 5% of the tektites are of the high-CaO type. However, at the M site (Maurasse 1991) which contains the least weathered spherules and where even the rim is preserved, 95% of the spherules contain a CaO-rich rim, with abundant skeletal melilite crystals. Thus the CaO-rich glass is at least as common as low-CaO dark glass. Water content is extremely low in the glass (<0.02%), being comparable to other tektites and impact glasses but unlike any known volcanic glass. The gas pressure in the abundant vesicles inside the glass is almost zero, as determined in crushing experiments, indicating that the glass was solidified in ballistic flight outside the atmosphere. Sm/Nd isotope compositions indicate target basement-rock model ages between 400 and 1100 Myr (Izett 1991), which is compatible with the Pan-African basement of Yucatan. The $\delta^{18}O$ composition of the yellow glass is compatible with a mixture of basement and limestone (Izett 1991). The $^{40}Ar/^{39}Ar$ ages of both the tektite glass and the melt sheet sample C1-N10 in the crater are indistinguishable at 65 Myr (Swisher et al 1992). The age, chemical, and isotopic compositions all strongly indicate that the impact glass from Haiti is derived from the Chicxulub crater.

The Beloc ejecta layer occurs in the Beloc formation, a sequence of well-bedded siliceous pelagic limestones and marls, overlying basaltic pillow lavas. Maurasse (1991) has shown that the Beloc formation and underlying basalts are obducted from the Caribbean ocean floor, and the original depth of deposition is >2000 m. The ejecta layer has a complex stratigraphy and is in most places redeposited, as a mass flow, and slump-folded. The two southernmost outcrops are the only deposits where the spherules still contain relict glass. In some sites the spherule layer is graded and often cross-bedded. The thickness of the layer varies from 12 cm to more than 70 cm. In the B site (Jehanno et al 1992) the layer crops out over >30 m and has a constant thickness of about 12 cm. In this site and the D site, the layer is imbricated in places by package gliding. I believe that the 12-cm thickness is close to the original thickness of the ejecta layer, not the >50 cm as reported elsewhere.

Iridium and shocked minerals are concentrated in the top of the layer (Jehanno et al 1992) (Figure 10) except in those locations where the ejecta layer is redeposited. In the H-site the iridium anomaly and spherule layer seem separated by 20 cm of normal limestone (Jehanno et al 1992). However, this limestone interval is cross bedded and sandy, comparable to the Bouma Tc-d interval in a turbidite.

DSDP Sites 536 (2790 m) and 540 (2926 m) are 420 and 530 km, respectively, northeast of the crater rim, probably too far from the crater to contain ejecta blanket diamictite below the iridium-rich ejecta deposits (Alvarez et al

1992b). Site 540 contains an unusually thick (2.6 m) unit of dark smectitic, cross-bedded, melt-clast breccia, grading upward. The top is enriched in iridium and shocked minerals (Figure 10). The cross bedding indicates that the melt-clast breccia is not primary fallout but transported in mass flow. The distribution of the melt clasts and the small nonmelted clasts is almost identical to the top of the ejecta sequence of borehole UNAM-5. The melt breccia in Site 540 is underlain by 45-m matrix-supported pebbly mudstone and in Site 536 by a poorly recovered 100 m interval of shallow-water grain stone fragments. These units indicate mass wasting from the Campeche platform margin, most likely caused by slope failure induced by the seismic energy of the impact.

Northern Belize and Southern Yucatan

On both sides of the Rio Hondo, ejecta-blanket deposits, discovered during the 1998 Planetary Society expedition, crop out in Albion Island (Ocampo et al 1996) and along the road from Chetumal to La Union. These outcrops with ejecta deposits are the nearest known to the Chicxulub crater, only 340 km from the crater center. The ejecta sequence is almost identical to that at Albion Island, but the sequence is more complete and overlying Paleocene sediments were also found (Figure 16). The ejecta sequence overlies the Barton Creek dolomite, a thick-bedded coarse dolomite with fossiliferous layers containing carcineretid crabs and *Nerinea* sp. of Maastrichtian age. The contact is an undulating, irregular surface, showing evidence for subaerial exposure (Pope et al, submitted to *Geology*). The basal layer, the spheroid bed of Ocampo et al (1996), follows this surface closely, and, although it rests on the highs or lows of the undulating contact, maintains an unusual constant thickness of about 1 m. The matrix consists of pulverized dolomite containing rounded dolomite clasts, deformed greenish clay blebs that may be the remains of glassy ejecta, and centimeter-sized, concentric banded dolomite spheroids. Internal layering is discontinuous. Large boulders do not occur, in contrast to the overlying diamictite bed. The overlying diamictite bed also has a dolomite matrix and contains dolomite boulders up to 10 m in size, some of which contain the same fossils as the underlying Barton Creek dolomite. Most of the large boulders are concentrated in the lower part. Smaller boulders and cobbles, the vast majority of dolomite, occur throughout the diamictite. The diamictite further contains about 20% of up to 4-cm large green droplets and blebs with internal vesicles, identical to altered impact glass in other proximal locations in the Gulf of Mexico region. A few subhorizontal shear zones occur, similar to shear zones found in the Bunte Breccia of the Ries crater. The diamictite is at least 30 m thick. Near Alvaro Obregon the diamictite is capped by a 15-cm-thick calcrete soil, a caliche, in turn overlain by 0.5 m of thin-bedded, fine-grained

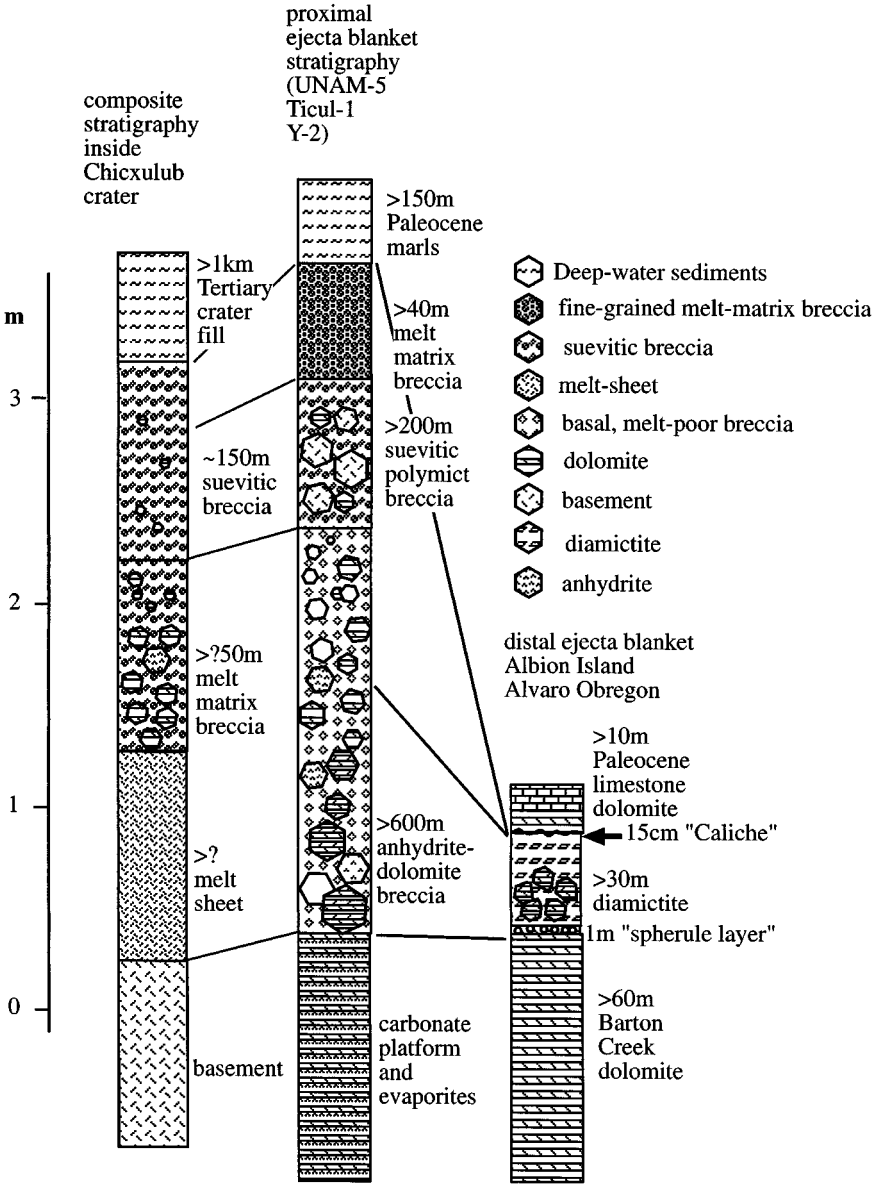

Figure 16 Reconstruction of the melt sheet and fall-back sequence in the Chicxulub crater, the proximal ejecta blanket sequence as known from drill holes Y-2, Ticul-1, and UNAM-5, and the more distal ejecta blanket sequence in Albion Island (Belize) and Alvaro Obregon in Mexico.

dolomite layers. The caliche layer is interpreted as a subaerial exposure of the ejecta, indicating that substantial erosion probably has removed the top of the ejecta sequence, prior to deposition of the dolomite beds. The thin-bedded dolomite grades into thin-bedded micritic limestones with a very small marine microfauna, ostracods, and foraminifers, probably representing a basal Paleocene transgressive sequence.

Pope et al (1998) suggest that the basal spheroid bed may represent the early blasts from the vapor plume. This may be true for some of the components, such as the vesicular clay blebs in the layer, but the presence of shear planes and slickensides, the constant thickness of the bed, the pulverized character of the matrix, and the layering in the bed indicate that this bed is produced by grinding during the horizontal movement of the ejecta curtain over the irregular karstic surface. The dolomite spheroids may have obtained their concentric banding by accretion within the layer, which is heated, and may be even partially melted through friction between the sliding ejecta curtain and authochtonous dolomite rather than from accretion in a turbulent, volatile-rich plume.

Ejecta In and Close to the Chicxulub Crater

Spot samples are recovered in the Chicxulub crater from drill cores Yucatan-6, Chicxulub-1, and Sacapuc-1 and just outside the crater in cores Y-1, Y-2, and Y-4. Shallow drill holes UNAM-5 and UNAM-6 (Marin & Sharpton 1994, Sharpton et al 1996, Hildebrand et al 1991) are continuously cored but penetrated only the top 300 m of the ejecta sequence. The stratigraphy of the ejecta is still preliminary, because the data are fragmentary and the results of further, continuously cored, deep drilling in the crater itself are awaited. Based on the seismic results of Morgan et al (1997), I believe the diameter of the crater to be 195 km.

The basal ejecta in the crater are holocrystalline igneous rocks, probably representing the almost clast-free impact melt sheet (C1-N9, 10). The $^{40}Ar/^{39}Ar$ age data from this melt sheet (Swisher et al 1992) show that the age of the melt is indistinguishable from the age obtained from impact glass at the K/T boundary in Beloc, Haiti, and Mimbral. Above the melt sheet is a melt-matrix breccia, dominated by melt clasts welded together and containing clasts of anhydrite and basement rocks up to 7 cm in size, often surrounded by coronas of augite. The overlying polymict suevitic breccias are graded from pebble to sand size, often containing reworked shallow-water biota of Cretaceous age and shocked minerals. The suevitic breccia is overlain by micritic pelagic sediments of Paleocene age. It is possible that between the melt-matrix breccia and the melt sheet a very coarse clastic unit occurs with >1-m-sized limestone, anhydrite, and dolomite boulders, considered by Meyerhoff et al (1994) to represent in situ anhydrite and limestone layers.

Just outside the crater, the stratigraphy of the ejecta curtain deposits (the basal part in particular) is poorly constrained. However, from the data from the T-1 and Y-2 wells from the base, and UNAM-5 and UNAM-6 from the top of the sequence, a stratigraphic sequence can be reconstructed (Figure 16).

The basal ejecta are presumably a coarse anhydrite and dolomite-clast breccia, with small amounts of melt clasts. The unit is >600 m thick, comparable and correlated to the diamictite bed of Albion Island (Sharpton et al 1996). The lack of anhydrite clasts in the Belizian diamictite and the similarity of the dolomite clasts to the underlying Barton creek dolomite suggest that the diamictite components in Belize may be derived from a local source, presumably by secondary cratering, rather than from the Chicxulub target rocks. These bunte breccia types of ejecta are overlain by a breccia unit rich in melt clasts and basement clasts that may be well over 300 m thick (UNAM-5). This dolomite/anhydrite breccia is overlain, with a sharp contact, by a >40 m (UNAM-5) sequence of ejecta that consists primarily (>90%) of melt clasts welded together and containing small <1-cm basement clasts and shocked grains. The melt clasts near the top display the familiar vesicles, and the size of the clasts decreases upward. The top of the sequence displays cross bedding, indicating that the ejecta clasts are now sand-sized, reworked, and transported by currents, presumably produced by seawater rushing back and filling the crater. A comparable cross-bedded melt clast unit occurs in the top of the ejecta sequence in DSDP Hole 540.

The ejecta blanket just south of the crater (UNAM-5) is overlain by micritic pelagic sediment, containing basal Paleocene nannofossils (J Pospichal, personal communication). On first sight, this might indicate that the area had subsided several hundred meters from near sea level on the evaporitic carbonate platform before the impact and suggests that the site would still be inside the topographic crater. However, its position in the graben, indicated by the gravity low extending south from the crater near the Ticul fault, indicates that this area may have been a deep-water trough before the impact (Figure 9). This pre-impact deep-water region may also be the source of the controversial deep-water Cretaceous planktonic foraminifers in the wash-back sediments above the ejecta in the crater (Lopez Ramos 1981, Meyerhoff et al 1994).

Although fragmentary, it appears that the stratigraphy of the proximal ejecta blanket is comparable to ejecta sequences observed near other impact craters, such as the Ries crater (Newsom et al 1990). Basically, the sequence represents the inverted stratigraphy of the impacted target rocks, with the melted basement rocks at the top of the sequence.

The ejecta blanket deposits extend somewhat beyond Albion Island (260 km, or 2.8 crater radii from the crater rim) but probably do not reach as far as middle

Belize (Pooks Hill) or El Caribe in Guatamala, 375 km and 430 km or 3.9 and 4.5 crater radii from the rim of the crater, respectively.

LOWERMOST PALEOCENE

The lowermost Paleocene sediments deposited directly above the ejecta layer record the first reactions of the biosphere to the consequences of the Chicxulub impact event. The first observation is the presence of a few-centimeters-thick detrital clay layer, the K/T boundary clay, directly on top of the ejecta. With the possible exception of the El Kef section, there is no transitional interval, that is, from carbonate-rich to carbonate-poor, indicating a gradual collapse of the oceanic ecosystems. The conclusion is that the primary production in the oceans was reduced suddenly and dramatically as a consequence of the impact event. This is supported by the negative $\delta^{13}C$ shift recorded globally in the first sediments above the ejecta layer. The thickness of the K/T clay layer corresponds to the sedimentation rate of clay in sediments deposited before and after the K/T boundary and ranges from 1 cm in the Apennines, 6.5 cm in Agost, and 10 cm in Caravaca, to 25 cm in El Kef. The length of time involved in deposition of the boundary clay layer, and by inference the length of the carbonate and primary production crisis in the oceans, can be extrapolated from the background clay sedimentation rates. Extrapolation from the Cretaceous, with higher clay flux than the basal Danian, yields a duration between 4000 and 8000 years, and extrapolation from the Danian yields a duration between 8000 and 16,000 years.

The boundary clay still has enhanced iridium concentrations, but these decrease exponentially upward. Diffusion, bioturbation, prolonged ocean residence times of iridium and redeposition from primary deposits are offered as explanations. The absence of any anomalous iridium in the boundary clay where the ejecta layer is missing, as in the Geulhemmerberg, Holland (Smit & Rocchia 1996), indicates no evidence for a prolonged supply of iridium.

The boundary clay contains a few other noteworthy clues. In the base of the clay, there is no confirmed record yet of new Paleocene species. The remaining biota are either reworked or surviving elements from the Cretaceous oceans.

Dinoflagellate cysts occur abundantly in the K/T boundary clay, and are so abundant that A Loeblich (personal communication) termed the Fish clay in Denmark a "dinoflagellate soup." Apparently, this group, which suffered no extinctions, flourished directly after the impact, and therefore its distribution and abundance patterns might yield clues about the environmental conditions of the oceans just after the impact, where groups such as nannoplankton and foraminifera have disappeared (Brinkhuis & Schioler 1996). One such clue is the immigration of *Palynodinium grallator*, a cool-water species from Denmark

in the Maastrichtian, in the basal boundary clay of El Kef (Brinkhuis et al 1998). This is the first empirical support for dust-cloud-cooling scenarios in the geological record. Subsequently, still in the base of the boundary clay, warm tropical species (*Trithynodinium evitii*, *Manumiella druggii*) migrated from the tropics to Denmark, which supports the earlier reported negative shift (Romein & Smit 1981) in $\delta^{18}O$ in the boundary clay that indicated a substantial warming of ocean surface water during deposition of the remainder of the boundary clay.

Some organic molecular markers, exclusively found in the basalmost part of the boundary clay, indicate a short, intense period of fermentation of massive amounts of organic matter on the seafloor in El Kef and Geulhemmerberg sections (J de Leeuw et al, unpublished data). This is the best indication so far for mass mortality following the impact event. Evidence of mass mortality was earlier suspected on the basis of abundant framboidal pyrite in the boundary clay and the leaching and dissolution of the top of the Maastrichtian.

New incoming species of both the planktic foraminifera and nannofossils occur in the top of the boundary clay. It is unclear whether reports of new species already in the boundary clay (Keller 1997) are due to the frequent ichnofossils penetrating from above and forming traces filled with younger material. The boundary clay in the Geulhemmerberg, which has no overlying strata with basal Paleocene species, however, contains exclusively Cretaceous survivor species.

Beyond the clear conclusion that the mass extinctions and mass mortality are closely linked to the Chicxulub impact event, it is not yet clear how the impact event is linked to the extinctions. Many suggestions have been offered, but the original suggestion of Alvarez et al (1980), that a short period of photosynthesis shutdown followed by a food-chain collapse in combination with a prolonged period (>3 kyr) of global warming, would explain most of the biotic events.

ACKNOWLEDGMENTS

During my investigations of the mass extinctions at the K/T boundary, I have benefited greatly from discussions and other contributions of many colleagues: A. Montanari, W. Alvarez, P. Claeys, Th. B. Roep, J. Van Hinte, H. Vonhof, T. v. Eijden, T. v. Kempen, G. Ganssen, G. Klaver, H. Brinkhuis, J. Jagt, P. Willekes, M. Konert, R. van Elsas, and numerous others. I thank S. Kars for the many excellent SEM graphs. Financial support is acknowledged of the Vrije Universiteit, The Netherlands Organization for Scientific Research (NOW), and the Royal Dutch Academy of Sciences (KNAW). This is NSG contribution No. 981002.

Literature Cited

Alvarez LW, Alvarez W, Asaro F, Michel HV. 1980. Extraterrestrial cause for the Cretaceous-Tertiary extinction. *Science* 208: 1095–108

Alvarez W, Grajales NJM, Martinez SR, Romero MPR, Ruiz LE, et al. 1992a. The Cretaceous-Tertiary boundary impact-tsunami deposit in NE Mexico. *Geol. Soc. Am. Abstr. Programs* 24:A331

Alvarez W, Smit J, Lowrie W, Asaro F, Margolis SV, et al. 1992b. Proximal impact deposits at the Cretaceous-Tertiary boundary in the Gulf of Mexico: a restudy of DSDP Leg 77 Sites 536 and 540. *Geology* 20:697–700

Berger A, Loutre MF, Dehant V. 1989. Influence of the changing lunar orbit on the astronomical frequencies. *Paleoceanography* 4:555–64

Berggren WA, Kent DV, Flynn JJ, Van Couvering JA. 1985. Cenozoic geochronology. *Geol. Soc. Am. Bull.* 96:1407–18

Berggren WA, Kent DV, Swisher CCS, Aubry M-P. 1995. A revised Cenozoic geochronology and chronostratigraphy. In *Geochronology, Time Scales and Global Stratigraphic Correlation*, Spec. Publ. 54:129–212. Tulsa, OK: Soc. Econ. Paleontol. Mineral.

Blum JD. 1992. Oxygen isotope constraints on the origin of impact glasses from the Cretaceous-Tertiary boundary. *Science* 257:1104–7

Bohor BF. 1996. A sediment gravity flow hypothesis for siliciclastic units at the K/T boundary, northeastern Mexico. In *The Cretaceous-Tertiary Event and Other Catastrophes in Earth History*, ed. G Ryder, D Fastovski, S Gartner, Spec. Pap. 307:183–96. Boulder, CO: Geol. Soc. Am. 569 pp.

Bohor BF, Foord EE, Modreski PJ, Triplehorn DM. 1984. Mineralogic evidence for an impact event at the Cretaceous-Tertiary boundary. *Science* 224:867–69

Bohor BF, Triplehorn DM, Nichols DJ, Millard HT. 1987. Dinosaurs, spherules and the "magic" layer: a new K-T boundary clay site in Wyoming. *Geology* 15:896–99

Bralower TJ, Paull CK, Leckie RM. 1998. The Cretaceous-Tertiary boundary cocktail: Chicxulub impact triggers margin collapse and extensive sediment gravity flows. *Geology* 26:331–34

Brinkhuis H, Schioler P. 1996. Palynology of the Geulhemmerberg Cretaceous/Tertiary boundary section (Limburg, SE Netherlands). In *The Geulhemmerberg Cretaceous/Tertiary Boundary Section (Maastrichtian Type Area, SE Netherlands)*, ed. H Brinkhuis, J Smit, Spec. Issue Geol. Mijnbouw 75:193–213. Dordrecht, The Netherlands/Norwell, MA: Kluwer Academic

Buffler RT, Schlager W, Bowdler JL, Cotillon PH, Halley RB, et al. 1984. *Initial Reports of the Deep-Sea Drilling Project*, Washington, DC: US Govt. Print. Off. 365 pp.

Carlisle BB, Braman DR. 1991 Nanometre size diamonds in the Cretaceous/Tertiary boundary clay of Alberta. *Nature* 352:708–9

Christensen L, Fregerslev S, Simonsen A, Thiede J. 1973. Sedimentology and depositional environment of lower Danish Fish clay from Stevns Klint, Denmark. *Bull. Geol. Soc. Denmark* 22:193–212

Cowie JW, Zieger W, Remane J. 1989. Stratigraphic Commission accelerates progress, 1984–1989. *Episodes* 112:79–83

Desor E. 1846. Sur le Terrain Danien, nouvel étage de la craie. *Bull. Soc. Geol. Fr.* 4:181

Fourcade E, Rocchia R, Gardin S, Bellier JP, Debrabant P, et al. 1998. Age of the Guatemala breccias around the Cretaceous Tertiary boundary: relationships with the asteriod impact on the Yucatan. *C.R. Acad. Sci. Paris* 327:47–53

Gartner S. 1996. Calcareous nannofossils at the Cretaceous-Tertiary boundary. In *Cretaceous-Tertiary Mass Extinctions*, ed. N Macleod, G Keller, pp. 27–48. New York: Norton

Glass BP, Burns CA. 1988. Microkrystites: a new term for impact-produced glassy spherules containing primary crystallites. In *Lunar and Planetary Science Conference*, ed. S Ryder, New York: Pergamon. 18:455–8

Groot JJ, de Jonge RBG, Langereis CG, ten Kate WGHZ, Smit J. 1989. Magnetostratigraphy of the Cretaceous-Tertiary boundary at Agost (Spain). *Earth Planet. Sci. Lett.* 94:385–97

Haq BU, Hardenbol J, Vail PR. 1988. *Mesozoic and Cenozoic Chronostratigraphy and Cycles of Sea-level Change*. Spec. Publ. 42:71–108. Tulsa, OK: Soc. Econ. Paleontol. Mineral.

Herbert TD, D'Hondt SL. 1990. Precessional climate cyclicity in Late Cretaceous-Early Tertiary marine sediments: a high resolution chronometer of Cretaceous-Tertiary boundary events. *Earth Planet. Sci. Lett.* 99:263–75

Hildebrand AR, Penfield GT, Kring DA, Pilkington M, Camargo ZA, et al. 1991. Chicxulub crater: a possible Cretaceous/Tertiary boundary impact crater on the Yucatán Peninsula, Mexico. *Geology* 19:867–71

Huber BT. 1992. Upper Cretaceous planktic foraminiferal biozonation for the austral realm. *Mar. Micropaleontol.* 20:107–28

Izett GA. 1990. The Cretaceous/Tertiary boundary interval, Raton Basin, Colorado and New Mexico, and its content of shock-metamorphosed minerals: evidence relevant to the K/T boundary impact-extinction theory. *Geol. Soc. Am. Spec. Pap.* 249:1–100

Izett GA. 1991. Tektites in Cretaceous-Tertiary boundary rocks on Haiti and their bearing on the Alvarez impact extinction hypothesis. *J. Geophys. Res.* 96:20879–905

Jehanno C, Boclet D, Froget L, Lambert B, Robin E, et al. 1992. The Cretaceous Tertiary boundary at Beloc, Haiti: no evidence for an impact in the Caribbean area. *Earth Planet. Sci. Lett.* 109:229–41

Kate WGT, Sprenger A. 1993. Orbital cyclicities above and below the Cretaceous/ Paleogene boundary at Zumaya (N Spain), Agost and Relleu. *Sediment. Geol.* 87:69–101

Keller G. 1988. Extinction, survivorship and evolution of planktic foraminifera across the Cretaceous/Tertiary boundary at El Kef, Tunisia. *Mar. Micropaleontol.* 13:239–63

Keller G. 1996. The Cretaceous-Tertiary mass extinction in planktonic foraminifera: biotic constraints for catastrophic theories. See Gartner 1996, pp. 19–84

Keller G. 1997. Analysis of El Kef blind test I. *Mar. Micropaleontol.* 29:89–93

Keller G, Lopez-Oliva JG, Stinnesbeck W, Adatte T. 1997. Age, stratigraphy, and deposition of near-K/T siliciclastic deposits in Mexico: relation to bolide impact? *Geol. Soc. Am. Bull.* 109:410–28

Keller G, Stinnesbeck W. 1996. Sea-level changes, clastic deposits, and mega tsunamis across the Cretaceous Tertiary boundary. See Gartner 1996, pp. 415–50

Keller G, Stinnesbeck W, Lopez-Oliva JG. 1994. Age, deposition and biotic effects of the Cretaceous/Tertiary boundary event at Mimbral, NE Mexico. *Palaios* 9:144–57

Kent DV. 1977. An estimate of the duration of the faunal change at the Cretaceous-Tertiary boundary. *Geology* 5:769–71

Klaver GT, Kempen TMG, Bianchi FR, Gaast SJ. 1986. Green spherules as indicators of the Cretaceous Tertiary boundary in DSDP Hole 603b. In *Initial Reports of the Deep Sea Drilling Project*, ed. JE VanHinte, W. Wise, 93:1039–55. Washington, DC: US Govt. Print. Off. 1205 pp.

Koeberl C. 1992. Watercontent of glasses from the K/T boundary, Haiti: an indication of impact origin. *Geochim. Cosmochim. Acta* 56:4329–32

Koeberl C, Sigurdsson H. 1992. Geochemistry of impact glasses from the K/T boundary in Haiti: relation to smectites and a new type of glass. *Geochim. Cosmochim. Acta* 56:2113–29

Kotake N. 1989. Paleoecology of the Zoophycos producers. *Lethaia* 22:327–41

Kring DA, Boynton WV. 1991. Altered spherules of impact melt and associated relic glass from the K/T boundary sediments in Haiti. *Geochim. Cosmochim. Acta* 55:1737–42

Kyte FT, Bostwick JA. 1995. Magnesioferrite spinel in Cretaceous/Tertiary boundary sediments of the Pacific basin: remnants of hot, early ejecta from the Chicxulub impact? *Earth Planet. Sci. Lett.* 132:113–27

Kyte FT, Bostwick JA, Zhou L. 1996. The Cretaceous-Tertiary boundary on the Pacific plate: composition and distribution of impact debris. See Bohor 1996, pp. 389–402

Kyte FT, Leinen M, Heath GR, Zhou L. 1993. Cenozoic sedimentation history of the central North Pacific: Inferences from the elemental geochemistry of core LL44-GPC3 *Geochim. Cosmochim. Acta* 57:1719–40

Lerbeckmo JF, Sweet AR, Duke MJM. 1996. A normal polarity subchron that embraces the K/T boundary: a measure of sedimentary continuity across the boundary and synchroniety of boundary events. See Bohor 1996, pp. 465–76

Lindinger M. 1989. *The Cretaceous Tertiary boundary in the Caravaca and Kef sections*. PhD thesis. ETH Zurich. 213 pp.

Lopez Ramos E. 1981. *Geologia de Mexico*. Mexico City: UNAM. 446 pp.

Luterbacher HP, Premoli Silva I. 1964. Biostratigrafia del limite cretaceo-terziario nell'Appennino centrale. *Riv. Ital. Paleontol. Stratigr.* 70:67–128

Lyons JB, Officer CB. 1992. Mineralogy and petrology of the Haiti Cretaceous/Tertiary section. *Earth Planet. Sci. Lett.* 109:205–24

Marin LE, Sharpton V. 1994. Recent drilling and core recovery within the Chicxulub impact structure, northern Yucatan, Mexico. *Eos, Trans. Am. Geophys. Union, Fall Meet.* 75(44):408–9 (Abstr.)

Maurasse FJMR. 1991. Impacts, tsunamis, and the Haitian Cretaceous-Tertiary boundary layer. *Science* 252:1690–93

Meyerhoff AA, Lyons JB, Officer CB. 1994. Chicxulub structure: a volcanic sequence of Late Cretaceous age. *Geology* 22:3–4

Michel HV, Asaro F, Alvarez W, Alvarez LW. 1985. Elemental profile of iridium and other elements near the Cretaceous/Tertiary boundary in Hole 577B. In *Initial Reports of the Deep-Sea Drilling Project*, ed GR Heath, LH Burckle, 86:533–38. Washington DC: US Govt. Print. Off. 689 pp.

Montanari A. 1990. Authigenesis of impact spheroids in the K/T boundary clay from Italy: New constraints for high-resolution

stratigraphy of terminal cretaceous events. *J. Sediment. Petrol.* 61:315–39

Montanari A, Claeys P, Asaro F, Bermudez J, Smit J. 1994. Preliminary stratigraphy and iridium and other geochemical anomalies across the KT boundary in the Bochil section (Chiapas, southeastern Mexico). In *New Developments Regarding the KT Event and Other Catastrophes in Earth History.* LPI Contrib. 825:84–85 (Abstr.) Houston: Lunar Planet. Inst.

Montanari A, Hay RL, Alvarez W, Asaro F, Michel HV, et al. 1983. Spheroids at the Cretaceous-Tertiary boundary are altered impact droplets of basaltic composition. *Geology* 11:668–71

Moreau MG, Cojan I, Ory J. 1994. Mechanisms of remanent magnetization in marl and limestone alternations. Case study: Upper Cretaceous (Chron 31-30), Sopelana, Basque Country. *Earth Planet. Sci. Lett.* 123:15–37

Moreau MG, Mary C, Orue Etxebarria X. 1989. Magnetostratigraphy of the Sopelana K/T boundary section. *Terra Abstr.* 1:254

Morgan J, Warner M, Brittan J, Buffler R, Camargo A, et al. 1997. Size and morphology of the Chicxulub impact crater. *Nature* 390:472–76

Nederbragt AJ, Koning JA. 1994. Morphologic variation in Turonian to Maastrichtian Heterohelix globulosa (Ehrenberg). *Proc. K. Ned. Akad. Wet.* 97:429–44

Newsom HE, Graup G, Iseri DA, Geissman JW, Keil K. 1990. The formation of the Ries crater, West Germany: evidence of atmospheric interactions during a large cratering event. In *Global Catastrophes in Earth History; An Interdisciplinary Conference on Impacts,Volcanism, and Mass Mortality*, ed. VL Sharpton, PD Ward, Spec. Pap. 247:195–206. Boulder, CO: Geol. Soc. Am. 631 pp.

Ocampo AC, Pope KO, Fisher AG. 1996. Ejecta blanket deposits of the Chicxulub crater from Albion Island, Belize. See Bohor 1996, pp. 75–88

Officer CB, Page J. 1996. *The Great Dinosaur Extinction Controversy.* Helix Books, Reading, MA: Addison-Wesley. 209 pp.

Olsson RK, Miller KG, Browning V, Habib D, Sugarman PJ. 1997. Ejecta layer at the Cretaceous-Tertiary boundary, Bass River, New Jersey (Ocean Drilling Program Leg 174AX). *Geology* 25:588–90

Oskarsson N, Helgason O, Sigurdsson H. 1996. Oxidation state of iron in tektite glasses from the Cretaceous Tertiary boundary. See Bohor 1996, pp. 445–52

Pardo A, Ortiz N, Keller G. 1996. Latest Maastrichtian and Cretaceous-Tertiary boundary foraminiferal turnover and environmental changes at Agost, Spain. See Gartner 1996, pp. 139–72

Percival SF, Fischer AG. 1977. Changes in calcareous nannoplankton in the Cretaceous-Tertiary biotic crisis at Zumaya, Spain. *Evol. Theory* 2:1–35

Pope KO, Ocampo AC, Fischer AG, Alvarez W, Fouke BW, et al. 1999. Proximal Chicxulub ejecta from Albion Island, Belize. *Geology.* (In press)

Robin E, Boclet D, Bonte P, Froget L, Jehanno C, et al. 1991. The stratigraphic distribution of Ni-rich spinels in Cretaceous-Tertiary boundary rocks at El Kef (Tunisia), Caravaca (Spain) and Hole 761C (Leg 122). *Earth Planet. Sci. Lett.* 107:715–21

Robin E, Froget L, Jehanno C, Rocchia R. 1993. Evidence for a K/T impact in the Pacific Ocean. *Nature* 363:615–18

Roggenthen WM. 1976. Magnetic stratigraphy of the Paleocene: a comparison between Spain and Italy. *Mem. Soc. Geol. Ital.* 15:73–82

Romein AJT, Smit J. 1981. Carbon-oxygen isotope stratigraphy of the Cretaceous-Tertiary boundary interval: data from the Biarritz section (SW France). *Geol. Mijnbouw* 60:541–44

Romein AJT, Willems H, Mai H. 1996. Calcareous nannoplankton of the Geulhemmerberg K/T boundary section, Maastrichtian type area, The Netherlands. See Brinkhuis & Schioler 1996, pp. 231–38

Ruiz FM, Huertas MO, Palomo I, Barbieri M. 1992. The geochemistry and mineralogy of the Cretaceous Tertiary boundary at Agost (southeast Spain). *Chem. Geol.* 95:265–81

Sharpton VL, Marin LE, Carney JL, Lee S, Ryder G, et al. 1996. A model of the Chicxulub impact basin based on evaluation of geophysical data, well logs and drill core samples. See Bohor 1996, pp. 55–74

Sigurdsson H, D'Hondt S, Arthur MA, Bralower TJ, Zachos JC, et al. 1991. Glass from the Cretaceous-Tertiary boundary in Haiti. *Nature* 349:482–87

Smit J. 1977. Discovery of a planktonic foraminiferal association between the Abathomphalus mayaroensis zone and the "Globigerina" eugubina zone at the Cretaceous/Tertiary boundary in the Barranco del Gredero (Caravaca, SE Spain): a preliminary report. *Proc. K. Ned. Akad. Wet.* 80:280–301

Smit J, Alvarez W, Claeys P, Montanari A, Roep TB. 1994. Misunderstandings regarding the KT boundary deposits in the Gulf of Mexico. See Montanari 1994, p. 116 (Abstr.)

Smit J, Alvarez W, Montanari A, Swinburne N, Kempen TM, et al. 1992a "Tektites" and microkrystites at the Cretaceous Tertiary bound-

ary: two strewnfields, one crater? *Proc. Lunar Planet. Sci. Conf.* 22:87–100
Smit J, Keller G, Zargouni F, Razgallah S, Shimi M, et al. 1997. The El Kef sections and sampling procedures. *Mar. Micropaleontol.* 29:69–72
Smit J, Montanari A, Swinburne NHM, Alvarez W, Hildebrand AR, et al. 1992b Tektite-bearing, deep-water clastic unit at the Cretaceous-Tertiary boundary in northeastern Mexico. *Geology* 20:99–103
Smit J, Nederbragt AJ. 1997. Analysis of the El Kef blind test II. *Mar. Micropaleontol.* 29:94–100
Smit J, Rocchia R. 1996. Neutron activation analysis of trace elements in the Geulhemmerberg Cretaceous/Tertiary boundary section, SE Netherlands. See Brinhuis & Schioler 1996, pp. 269–74
Smit J, Roep TB, Alvarez W, Montanari A, Claeys P, et al. 1996. Coarse grained, clastic sandstone complex at the K/T boundary around the Gulf of Mexico: deposition by tsunami waves induced by the Chicxulub impact? See Bohor 1996, pp. 151–82
Smit J, Romein AJT. 1985. A sequence of events across the Cretaceous-Tertiary boundary. *Earth Planet. Sci. Lett.* 74:155–70
Stinnesbeck W, Barbarin JM, Keller G, Oliva JGL, Pivnik DA, et al. 1993. Deposition of channel deposits near the Cretaceous-Tertiary boundary in northeastern Mexico: catastrophic or "normal" sedimentary deposits? *Geology* 21:797–800
Stinnesbeck W, Keller G. 1996. K/T boundary coarse-grained siliciclastic deposits in northeastern Mexico and northeastern Brazil: evidence for mega-tsunami or sealevel changes? See Bohor 1996, pp. 197–210
Stinnesbeck W, Keller G, Adatte T, Oliva JGL, MacLeod N. 1996. Cretaceous-Tertiary boundary clastic deposits in northeastern Mexico: impact tsunami or sealevel lowstand? See Gartner 1996, pp. 471–518
Stinnesbeck W, Keller G, Cruz J, Leon C, MacLeod N, et al. 1997. The Cretaceous-Tertiary transition in Guatemala: limestone breccia deposits from the South Péten basin. *Geol. Rundsch.* 86:686–710
Swisher CC III, Nishimura JMG, Montanari A, Pardo EC, Margolis SV, et al. 1992. Coeval 40Ar/39Ar ages of 65.0 million years ago from Chicxulub crater melt-rock and Cretaceous-Tertiary boundary tektites. *Science* 257:954–58
Van Andel TH, Thiede J, Sclater JG, Hay WW. 1977. Depositional history of the South Atlantic Ocean during the last 125 million years. *J. Geol.* 85:651–98
Worsley T. 1974. The Cretaceous-Tertiary boundary event in the ocean. In *Studies in Paleoceanography*, ed. WW Hay, Spec. Publ. 20:94–125. Tulsa, OK: Soc. Econ. Paleontol. Mineral. 235 pp.

Annual Review of Earth and Planetary Science
Volume 27, 1999

CONTENTS